RIVER HYDRO- AND MORPHODYNAMICS: RESTORATION, MODELING, AND UNCERTAINTY

by

Ari Joseph Posner

A Dissertation Submitted to the Faculty of the

DEPARTMENT OF HYDROLOGY AND WATER RESOURCES

In Partial Fulfillment of the Requirements
For the Degree of

DOCTOR OF PHILOSOPHY
WITH A MAJOR IN HYDROLOGY

In the Graduate College

THE UNIVERSITY OF ARIZONA

2011

THE UNIVERSITY OF ARIZONA
GRADUATE COLLEGE

As members of the Dissertation Committee, we certify that we have read the dissertation prepared by Ari J. Posner

entitled River Hydro- and Morphodynamics: Restoration, Modeling, and Uncertainty

and recommend that it be accepted as fulfilling the dissertation requirement for the Degree of Doctor of Philosophy

_____ Date: 11/30/2011
Jennifer G. Duan

_____ Date: 11/30/2011
Victor R. Baker

_____ Date: 11/30/2011
Kevin E. Lansey

_____ Date: 11/30/2011
Hoshin V. Gupta

Final approval and acceptance of this dissertation is contingent upon the candidate's submission of the final copies of the dissertation to the Graduate College.

I hereby certify that I have read this dissertation prepared under my direction and recommend that it be accepted as fulfilling the dissertation requirement.

_____ Date: 11/30/2011
Dissertation Director: Jennifer G. Duan

STATEMENT BY AUTHOR

This dissertation has been submitted in partial fulfillment of requirements for an advanced degree at the University of Arizona and is deposited in the University Library to be made available to borrowers under rules of the Library.

Brief quotations from this dissertation are allowable without special permission, provided that accurate acknowledgment of source is made. Requests for permission for extended quotation from or reproduction of this manuscript in whole or in part may be granted by the head of the major department or the Dean of the Graduate College when in his or her judgment the proposed use of the material is in the interests of scholarship. In all other instances, however, permission must be obtained from the author.

SIGNED: Ari J Posner

ACKNOWLEDGMENTS

First and foremost I would like to that Dr. Jennifer Duan for her timeless mentoring, profound scientific insights, and unending support, encouragement, and motivation. Only through her hours of discussion with me could any of this work been accomplished and I am forever indebted. I would also like to thank other professors who mentored me through this endeavor and went above and beyond the call of duty in their teaching efforts, including: Vince Tidwell, Hoshin Gupta, Victor Baker, Kevin Lancey, Tom Meixner, and Ty Ferre.

The financial support of Sandia National Laboratories, the Salt River Project, and the UA Peace Corps Fellows was critical in allowing me the opportunity to pursue this work and provide a spring board to my career as a geoscientist.

Finally, I would like to thank my family, by blood and by choice, for their support and encouragement through this stupendous test of my resolve, commitment, and wear-with-all. I could not have done this without you.

Thank you all so much.

TABLE OF CONTENTS

LIST OF TABLES

ABSTRACT

The study of fluvial geomorphology is one of the critical sciences in the 21st Century. The previous century witnessed a virtual disregard of the hydro and morphodynamic processes occurring in rivers when it came to design of transportation, flood control, and water resources infrastructure. This disregard, along with urbanization, industrialization, and other land uses has imperiled many waterways. New technologies including geospatially referenced data collection, laser-based measurement tools, and increasing computational powers by personal computers are significantly improving our ability to represent these complex and diverse systems. We can accomplish this through both the building of more sophisticated models and our ability to calibrate those models with more detailed data sets. The effort put forth in this dissertation is to first introduce the accomplishments and challenges in fluvial geomorphology and then to illustrate two specific efforts to add to the growing body of knowledge in this exciting field.

First, we explore a dramatic phenomenon occurring in the Middle Rio Grande River. The San Marcial Reach of the Rio Grande River has experienced four events that completely filled the main channel with sediment over the past 20 years. This sediment plug has cost the nation millions of dollars in both costs to dredge and rebuild main channels and levees, along with detailed studies by engineering consultants. Previous efforts focused on empirical relations developed with historical data and very simple one dimensional representation of river hydrodynamics. This effort uses the state-of-the-art three-dimensional hydro and morphodynamic model Delft3D. We were able to use this model

to test those hypotheses put forth in previous empirical studies. We were also able to use this model to test theories associated with channel avulsion. Testing found that channel avulsions thresholds do exist and can be predicted based on channel bathymetric changes.

The second effort included is a simple yet sophisticated model of river meander evolution. Prediction of river meandering planform evolution has proven to be one of the most difficult problems in all of geosciences. The limitations of using detailed three dimensional hydro and morphodynamic models is that the computational intensity precludes the modeling of large spatial or temporal scale phenomenon. Therefore, analytical solutions to the standard Navier-Stokes equations with simplifications made for hydrostatic pressure among others, along with sediment transport functions still have a place in our toolbox to understand and predict this phenomenon. One of the most widely used models of meander propagation is the Linear Bend Model that employs a bank erosion coefficient. Due to the various simplifications required to find analytical solutions to these sets of equations, efforts to build the stochasticity seen in nature into the models have proven useful and successful. This effort builds upon this commonly used meander propogation model by introducing stochasticity to the known variability in outer bank erodibility, resulting in a more realistic representation of model results.

1. INTRODUCTION

1.1 Explanation of the Problem and Its Context

Fluvial geomorphology is the study of sediment sources, fluxes and storage within the river catchment and channel over short, medium, and longer timescales and of the resultant channel and floodplain morphology (Newson and Sear, 1993). Over the past two decades, river management policy and practice have identified the application of fluvial geomorphology as critical to addressing the financial and environmental costs of ignoring natural system processes and structure in river management (Evans et. al., 2002). Applied fluvial geomorphology is concentrated on answering three questions (Sear and Newson, 2010)

1. How is the problem linked to the catchment sediment system?
2. What are the local geomorphological factors that contribute to the problem?
3. What is the impact of any proposed/existing solutions on channel geomorphology, including physical habitat and sediment transport processes?

Attempts to understand the Earth's physical processes rely on studying three components, causes, effects, and laws. Causes and effects can also be thought of as independent and dependent variables, respectively. Natural laws are the relationships among those variables. Table 1 lists some of those components used in fluvial geomorphology.

Table 1. Variables commonly used in fluvial geomorphology studies.

Independent Variables (Causes)	Dependent Variables (Effects)	Laws
Precipitation	Water Discharge	Laws of Motion
Temperature	Sediment Transport	Conservation of Mass
Valley Slope	Channel Width	Conservation of Energy

Sediment Size	Channel Depth	Conservation of Momentum
Geology	Channel Slope	Reduction/Oxidation
Pedology	Sinuosity	

These components are fit in to one of three logical explanation structures. Earth scientists use these structures to explain physical phenomena and attempt to understand how they relate to one another, so as to predict future outcomes.

1. *Deduction* is when initial conditions (causes) are used in combination with laws of nature to predict effects. Although deduction is a solid form of logic, the choice of relevant laws included in the model, the inclusion of generalizations rather than laws, numerical issues, and the initial and boundary conditions for the model which must be based on measurements that may be incomplete or contain errors are all significant limitations (Oreskes et al., 1994).

2. *Induction* is the use of statistical generalizations based on both causes and effects. An often used example is the hydraulic geometry relations used to relate discharge and cross-sectional properties of natural river channels (Ferguson, 1987). These relations are limited in that relations are only valid in those systems where data is collected and it is impossible to collect enough data to make universally valid generalizations.

3. *Abduction* can be thought of as the opposite of deduction. In abduction the final conditions (effects) are combined with laws to arrive at a hypothesis that explains the observations (Kleinhans, 2010). In many cases, abduction is used to explain present day landforms with a combination of hypotheses. The major limitation being that the correct hypothesis may not have been considered.

Despite our best efforts to understand fluvial systems a number of factors make conclusive explanations elusive. Some of the difficulties include (1) that fact that measurement techniques often disturb the observed process, (2) the timescale of our observations is much shorter than the phenomenon being studied, (3) many processes and phenomenon cannot yet be observed directly or indirectly, and (4) the fact that many fluvial processes have an intrinsic random or chaotic component (Klienhans, 2010). Nevertheless, much advancement exists in understanding these complex and dynamic systems.

1.2 Literature Review

The body of knowledge related to fluvial geomorphology goes back centuries, efforts to describe and understand these phenomenon date back to Leonardo de Vinci (Gyr 2010). Most morphodynamic research was carried out in humid regions, and it has been argued that those results should not be extrapolated to the arid and semi-arid zones (Finlayson and McMahon, 1988).

Catchment-scale processes in the semi-arid regions of the southwestern US and northern Mexico are very distinctive. Precipitation regimes are clearly segmented into winter and summer events. Summer events being characterized by localized and highly intense storms, where winter rains are of longer duration and less intensity. Several researchers have found that light winter rains produce significantly less runoff than summer thunderstorms (Brown, 1983; Wells, 1976). However, Thomsen and Schumann (1968) found that in Sycamore Creek 90 percent of runoff was generated during the winter

months. They attributed this to higher soil moisture content and reduced vegetation activity. Sources of streamflow in the arid southwest are highly variable from year to year and in different locations. The importance of winter snowpack, winter precipitation, and summer thunderstorms will vary in different catchments and locations within the catchment.

Semi-arid regions are also characterized by ephemeral channels with large transmission losses. Along Walnut Gulch (Tombstone, AZ), two flumes 10.9km apart recorded a loss of 57% during a single storm event (Renard and Keppel, 1966). The diversity of precipitation regimes, the differences in upland and lowland forcing controls (Table 2), and the diversity of vegetation communities in the arid southwest make setting the context of a stream reach critical to understanding the channel forming processes.

Table 2. Controls on river channel form in upland and lowland river channels.

Channel Controls	**Upland river**	**Lowland river**
Inflow Hydrograph	Flashy; steep *flood frequency curve*; snowmelt effects	Longer Duration Floods, moderate flood frequency curve; floods regulated by structures
Inflow Sediment	Bed material dominates; local sediment sources; forest and reservoir effects	Suspended load dominates; bank erosion or upland sources; Quality problems
Valley Slope	Steep; narrow	Gentle; wide. Floodplain effects on secondary flows and stream power.
Bed/bank materials	Coarse, cohesive, but also loose gravels	Fine, cohesive, engineered
In-stream vegetation	Little morphological role	Large seasonal impact on sediment transport
Riparian Vegetation	Sparse or short in headwaters	Often impacts from land conversion or use.
Section Geometry	Extremes of width/depth ratio	Low width/depth ratio in cohesive alluvium. Engineered changes

Long Profile	Steep, stepped; frequent instability zones and flood impacts often local	Gentle, often controlled by structure of seasonal vegetation growth
Planform	Full range present; most dynamic unless confined by cohesive soils, rock, or engineered structure	Confined, engineered, sinuous.

1.2.1. Channel Forming Processes

Channel form is the synthesis of factors at several spatial scales. In order to distinguish controls on channel form it is convenient to define a stream reach as 'the unit of river length in which the characteristics sources and sinks for sediments can be observed; as a result, the reach has a characteristic morphology: both geometry and form (Newson and Newson, 2000).'At the reach scale channel planform has been categorized by many researchers. The most referenced categories are likely those put forth by Leopold and Wolman (1957) that distinguish straight, braided, and meandering classes. Several other channel patterns were later proposed including anastomosing, anabranching, and wandering, among others. The categories put forth are related to specific parameters in the stream system such as, the dominance of suspended versus bedload sediment transport, low to high flow strength, small to large width/depth ratios, and high to low pattern stability (Schumm, 1968). Leopold and Wolman (1957) emphasized that natural rivers are a continuum of pattern classifications and Alabyan and Chalov (1998) showed that every natural pattern is a combination of the three main configurations listed above. Among all the classification efforts two classes of factors emerge that control channel pattern: flow strength and sediment characteristics.

An ongoing debate persists about the explanation for why certain patterns occur under different conditions. Classical explanations propose that channel pattern is a function of flow

strength, which can be represented by *Stream Power*, and sediment type and supply (Leopold and Wolman, 1957, Ferguson 1987, van den Berg, 1995). Contemporary explanations include the effects of cohesion of floodplains (Nanson and Croke, 1992), the width/depth ratio of the channel and the development of channel bars (Parker, 1976), the sorting of bed sediments and their particle size distribution (see Powell, 1998, for a review), the differences in mobility of particle sizes and the role of "hiding", where smaller particles are hidden in the lee of larger particles (Vollmer and Klienhans, 2008), particle sorting (Blom, 2008), and finally downstream fining where rivers progress from gravel to sand (Wright and Parker, 2005). In general, at least for perennial flows, channel dimensions are due mainly to water discharge, whereas shape and pattern are related to the type and quantity of sediment load (Cooke et. al., 1993).

Ferguson (1987) qualitatively clarified that the ratio of bank strength to flow strength can be used to explain observations of channel pattern, while Nanson and Croke (1992) used floodplain cohesion to distinguish channel patterns. The role of floodplains and bank strength is commensurate with sediment supply and particle size, as floodplains and banks are the sources of sediment supply. Riparian vegetation dramatically increases the cohesion of banks, reducing bank failure which is an important source of sediment. Riparian vegetation on floodplains increases the roughness of those areas, reducing stream velocities and thereby erosion potential.

Bank stability is a function of both vegetation and particle size. Stream banks are characterized by finer particle sizes than channel bottoms (Wells, 1976). Bank failure may result in river straightening and braiding, as sinuosity has been found to decrease with increasing proportions of silt and clay or vegetation in the channel banks and bed (Kleinhans, 2010).

The dynamics of sediment supplies in semi-arid regions are unique due to the dominance of ephemeral streams, the variability in precipitation, and heterogeneity of vegetation density. Perennial river channel morphology may conform to classifications in more humid regions; however, local ephemeral tributaries may play a major role. Debris flows, generated by tributaries of the Colorado River, for example, provide massive, largely immovable, boulders that create rapids and important hydraulic controls. The debris fans that ephemeral channels create constrict flow and deflect it to one side creating beaches up and downstream of the rapids and downstream debris bars in the main channel (Webb et. al., 1987).

Some other distinctive features that have been identified in drylands include:

1. High drainage density most likely due to the absence of dense vegetation cover, allowing for more linear erosion resulting channel development.
2. Channel networks are not fully integrated due to the localized nature of precipitation events leading to “hanging” tributaries which may block or deflect flow.

3. Channel networks have distinctive patterns. In hilly or mountainous bedrock areas, the innate geological structure is imposed on the pattern. In low-angle sparsely vegetated areas, the drainage pattern is usually pinnate or dendritic.
4. Where perennial streams have a concave upward long profile, ephemeral streams long profile is either flat or convex due to declining discharge downstream and increasing particle size (Brown 1983).
5. Channel adjustment appears to be relatively rapid, partly due to sparsity of riparian vegetation and intensity of storms (Cooke et. al., 1993).

While the particle size distribution and amount of sediment available to the stream are relatively straightforward concepts, despite the difficulty in defining a 'representative' particle size (Kliehhans, 2010), the channel forming discharge is more complex. Classical explanations of channel forming discharge use the *bankfull discharge*.

Bankfull discharge, a hydrologic term, is the flow rate when the stage of a stream is coincident with the uppermost level of the banks -- the water level at channel capacity, or bankfull stage. Bankfull stage is a fluvial-geomorphic term requiring an interpretation of site-specific landforms. In this context, bank typically refers to a sloping margin of a natural, stream-formed, alluvial channel that confines discharge during non-flood flow. Although the term bankfull stage can refer to various channel-bank levels, it generally applies to alluvial-stream channels (1) having sizes and shapes adjusted to recent fluxes of water and sediment, (2) that are principal conduits for discharges moving through a length of alluvial bottomland, and (3) that are bounded by flood plains upon which water

and sediment spill when the flow rate exceeds that of bankfull discharge. Thus, the concept of bankfull discharge, which often approximates the mean annual flood for perennial streams, includes the flood plain as a unique, identifiable geomorphic surface, all higher surfaces of alluvial bottomlands being terraces, and acknowledgement that bankfull discharge occurs only when stream stage is at flood-plain level.

1.2.2. Geomorphic Equilibrium

The concepts of a dynamic equilibrium in open channel flow by Leopold and Maddock (1953) and Mackin (1948) replaced the unsatisfactory notion of evolution of landforms borrowed from biology. The determination that river systems are in a dynamic or quasi equilibrium evolved from the finding of consistent patterns, or adjustments, in the relationships of stream width, depth, velocity, and sediment load. These observations, and the equilibrium concept, were later developed in terms of energy inputs, efficiency of utilization, and rate of entropy gain (Leopold and Langbein, 1962).

The energy that drives channel processes comes from the valley gradient which is the product of historic geological processes, commonly fluvial, glacial, and tectonic (Schumm 1977). The valley gradient then is not a product of the modern day river, but a condition imposed on the present river and one that it must adjust to depending on the water flow and sediment loads from upstream.

Geomorphologists use the Second Law of Thermodynamics to explain the equifinality of fluvial systems, where similar planforms occur under very different conditions. The

Second Law, or Law of Entropy, states that available energy in a system is always being converted to unavailable energy. Stated another way, a system will always go from order to disorder, an increase in entropy. In classical mechanics, in a closed system there can never be a decrease in entropy. However, most geomorphic systems are 'open' and can be thought of as dissipative systems where energy conversion can result in multiple forms (Hugget, 1986)

The balance between resisting and driving forces in fluvial system adjustment to equilibrium conditions is best summarized in Lane's Relation (1955). This figure illustrates the balance of forces and whether the stream will aggrade or degrade based on changes in discharge, sediment transport, bed slope, mean grain size, and changes to hydraulic roughness.

Concepts of stream power and changes to climatic inputs were used by Schumm (1968, 1969) to describe the metamorphosis of channels in the semi-arid riverine plain of the Murrumbidgee River in New South Wales, Australia. These relations summarize the changes that have occurred in the geologic record, but can also be used to predict changes likely to occur with changing boundary conditions.

$$Qw^{+} \backsimeq \frac{w^{+}d^{+}L^{+}}{S^{-}}$$

$$Qw^{-} \backsimeq \frac{w^{-}d^{-}L^{-}}{S^{+}}$$

$$Qs^{+} \backsimeq \frac{w^{+}L^{+}S^{+}}{d^{-}P^{-}}$$

$$Qs^{-} \backsimeq \frac{w^{-}L^{-}S^{-}}{d^{+}P^{+}}$$

Here a (+) sign indicates an increase in the variable and a (-) a decrease. Changes to water discharge (Qw), bedload sediment discharge (Qs), width (w), depth (d), meander wavelength (L), channel gradient (S), and sinuosity (P) are related to each other qualitatively.

While principles of minimum energy and stream power can give us great insights into the processes that generate different planforms, river restoration practitioners should be cautious of relying on these relations, primarily due to the temporal and spatial scales upon which they rely. Changes to geomorphic systems fall into two categories: persistent or semi-permanent changes in boundary conditions or environmental context (i.e. climate cycles) or singular discrete disturbances (i.e. volcanic eruption). However, the same phenomenon can be treated as either. For example, wildfire can be thought of as a discrete event or a shift to a new fire regime. Therefore, concepts of geomorphic changes and responses are linked to a combination of the intrinsic nature of the changes, the scale of the analysis of the problem, and the philosophical/methodological stance of the geomorphologist (Phillips, 2009).

Distinct assemblages of channel and floodplain geomorphic units provide insights into river behavior at the reach scale. Assemblages of bars, riffles, and pools, floodplains, etc. reflect both the contemporary form-process relationships as flow-depth relationships produce and rework distinct features, and the reach history as interpreted from the

distribution of remnant features such as ridge and swale topography, abandoned channels, and terraces. Small-scale bedforms are determined primarily by conditions experienced in the waning stage of the most recent bed deforming flow (Brierly and Fryers, 2005).

Semi-arid streams may be highly dynamic; however, if they return to consistent patterns and rates of change over hundreds to thousands of years, they are said to be geomorphologically stable. A stream is considered unstable if it exhibits abrupt, episodic, or progressive changes in position, geometry, gradient, or pattern that are anomalous or accelerated (Shields et. al., 2003). The distribution of forcing factors that drive river changes may be local (i.e., a landslide), regional (i.e., a storm), or continental (i.e., glaciation). Adjustments to the balance of impelling and resisting forces determine the reach planform. However, these are not simple cause and effect relationships. The *complex response* of fluvial systems may result in no response, short-lived effects, be part of a progressive change, instantaneous change, or a lagged response.

The main challenge in predicting river morphology is to distinguish the observed changes in terms of changes occurring in the entire catchment system versus the reach of interest (spatial-scale) and changes occurring as a result of intrinsic boundary conditions or extrinsic, human induced, forcing. As stated above, channel processes and forms are a result of both imposed and flux boundary conditions, previously stated arguments suggest there is a threshold condition for each river reach to pass from one planform type to another. Therefore, in cases where boundary conditions have changed such that

thresholds were overcome and planforms altered, it may not be feasible to return to, or restore, previous states. The temporal and spatial distribution, frequency, and timing of change indicate changes in both flux and imposed boundary conditions.

1.3. Explanation of Dissertation Format

This dissertation is the result of two major efforts put forth to describe, characterize, and predict geophysical phenomenon associated with alluvial rivers. The first paper is an effort to describe and predict the plugging of an alluvial river that is highly managed and is a major drainage of the semi-arid southwestern United States, the Rio Grande. This investigation is done using a state-of-the-art three-dimensional hydro- and morphodynamic model recently released to the research community as open source, Delft3D. The second effort described herein is more theoretical in nature, but with a profound potential for application. The effort is to build upon a quasi two-dimensional model of river meandering, incorporating stochasticity into the model representation. River meander prediction has a long history, has proven to be one of nature's most difficult phenomena to predict, and has numerous application to nature and society.

2. PRESENT STUDY

The methods, results, and conclusions of this study are presented in the papers appended to this dissertation. The following is a summary of the most important findings in the document.

2.1. River Avulsion and Main Channel Conveyance Loss

Main channel conveyance loss, such as that found in the Middle Rio Grande, are hydrodynamically complex and characterized by rapid morphologic changes. Because of the complex nature of this phenomenon it is still poorly understood. A numerical model based on the open source Delft3D flow model reproduces these complex hydrodynamics and morphodynamics reasonably well, in a qualitative sense. From model simulation results and available observations we conclude that:

- Numerical simulations of the hydro- and morphodynamics of the sediment plug phenomenon requires the presence of a non-cohesive sediment fraction in the suspended and bed sediment loads, that is commonly left out of morphodynamic modeling in alluvial rivers.
- Overbank flow, associated with spring snow melt, results in localized scour in floodplain areas that become conduits for increasing proportions of discharge, reducing the flow rate and sediment transport capacity of the main channel. This interrelationship is cyclic, and eventually the main channel becomes completely plugged.
- Channel avulsion is the cause of plugging of the main channel and not vice versa. Aggradation and perching of the main channel result in increasing ratios of both

main channel to floodplain height and the downstream or existing slope to the avulsion or new channel slope. Downstream of those areas that experience high ratios of both of these morphometric variables, significant main channel conveyance is lost. Although slope stability appears to be a better predictor of avulsion, the commensurate loss of main channel depth and increase in floodplain depth occurs in areas where channel perching is not significant.

- The impact of floodplain width on morphodynamics is much greater than the impact of main channel width. Dramatic morphologic changes occur during floodplain flow. Main channel geometry and its relation to the floodplain influence the preferential flow paths of moving water and sediment; however, floodplain geometry and the placement of the main channel in that context is more highly influential in determining morphologic changes during high flow events.

2.2. Stochasticity in Meander Modeling

This paper reports a quasi two-dimensional numerical simulation of meandering evolution using deterministic and stochastic models. The 1st order solutions of Navier Stokes equation in the curvilinear coordinate by Ikeda et al. (1981) and Johannesson and Parker (1989b) were used for determining the excess velocity. The rate of bank erosion is assumed linearly proportional to near bank excess velocity. The deterministic model adopted a constant coefficient of bank erosion for the entire simulation reach, whereas the stochastic model treated the coefficient of bank erosion as a random variable satisfying either uniform or normal distribution. For the deterministic model, Johannesson and

Parker (1989)'s model predicted better bend characteristics than the results of Ikeda et al. (1981)'s model although errors from both models exceeds 50%. This strongly suggested the limitation and incapability of deterministic models. On the other hand, the stochastic model yielded a 95% confidence interval bound that nearly encompasses 90% of the observed channel centerline. These results indicated that implementation of the Monte Carlo approach when using the suite of linear models is a more accurate representation of the evolution of the river planform and captures the variability associated with planform evolution and model error.

REFERENCES

Alabyan, A. and Chalov, R. (1998) Types of river channel patterns and their natural controls. Earth Surface Processes and Landforms 23, 467–74.

Blom, A. (2008) Different approaches to handling vertical and streamwise sorting in modeling river morphodynamics. Water Resources Research 44, W03415, DOI: 10.1029/2006WR005474.

Brierley, G.J. and Fryiers, K.A. (2005) Geomorphology and River Management: Application of the River Styles Framework. Blackwell Publishing, Australia.

Briggs, M. and Osterkamp, W.R. (2003) Important concepts for riparian recovery. Southwest Hydrology, March/April 2003. SAHRA, University of Arizona

Brown, A.J. (1983) Channel changes in arid badlands, Borrego Springs, California. Physical Geography, 4, 82-102.

Chapman, D., Codrington, S., Blong, R., Dragovich, D., Smith, T.L., Linacre, E., Riley, S., Short, A., Spriggs, J., and Watson, I. (1985) Understanding our earth. Pitman Publishing, Victoria.

Church, M. (2006) Bed material transport and the morphology of alluvial river channels. Annual Review of earth and Planetary Sciences 34, 325-54.

Cooke, R.U., Warren, A., and Goudie, A.S. (1993) Desert Geomorphology. UCL Press Ltd. London.

Dalrymple, Tate, and Benson, M.A., (1967) Measurement of peak discharge by the slope-area method: USGS—TWRI Book 3, Chapter A2, 12 p.

Evans, E.P., Ramsbottom, D.M., Wicks, J.M., Packman, J.C. and Penning-Roswell, E.C. (2002) Catchment flood management plans and the modellling and decision support framework. Civil Engineering, 150(1), 43-48.

Ferguson, R. (1987) Hydraulic and sedimentary controls of channel pattern. In Richards, K., editor, River channels: environment and process, Institute of British Geographers Special Publication 18, Oxford: Blackwell, 129–58.

Finlayson, B.L. and McMahon, T.A. (1988) Australia vs the world: a comparative analysis of streamflow characteristics. In Warner, R.J. (ed) Fluvial Geomorphology of Australia. Academic Press, Sydney, pp. 17-40.

Gordon, N.D., McMahon, T.A., Finlayson, B.L., Gippel, C.J. and Nathan, R.J. (2004) Stream Hydrology: An Introduction for Ecologists. John Wiley & Sons Ltd. West Sussex.

Gyr, A. (2010) The Meander Paradox-A Topological View. Applied Mechanics Reviews. Vol. 63, 020801-1-020801-12.

Huang, H.Q, Chang, H.H. and Nanson, G.C. (2004). Minimum energy as a hydrodynamic principle and as an explanation for variations in river channel pattern. Water Resources Research, W04502, 2004.

Huang, H. Q., and G. C. Nanson (2000), Hydraulic geometry and maximum flow efficiency as products of the principle of least action, Earth Surf. Processes Landforms, 25, 1 –13.

Huang, H. Q., and G. C. Nanson (2001), Alluvial channel-form adjustment and the variational principle of least action, in Proceedings of XXIX IAHR Congress, Beijing, pp. 410– 415, Int. Assoc. for Hydraul. Res., Delft, Netherlands.

Huang, H. Q., and G. C. Nanson (2002), A stability criterion inherent in laws governing alluvial channel flow, Earth Surf. Processes Landforms, 27, 929– 944.

Hugget, R.J. (1988) Dissipative systems: Implications for geomorphology. Earth Surface Processes and Landforms. Vol. 13, 45-49.

Hupp, C. R., (1986) The headward extent of fluvial landforms and associated vegetation on Massanutten Mountain, Virginia: Earth Surface Processes and Landforms, v.11, p. 545-555.

Ikeda, S., Parker, G. and Sawai, K., (1981) Bend theory of river meanders: Part I, Linear development. J. of Fluid Mech., 112, 363-377.

Jackson, L.L., Lopoukhine, N., and Hillyard, D. (1995) Ecological Restoration: A definition and comments. Restoration Ecology 3, 71-75.

Johannesson, H., and Parker, G., (1989) Velocity redistribution in meandering rivers. J. Hydraul. Eng., 115(8), 1019-1039.

Kleinhans, M.G. (2010) Sorting out river channel patters. Progress in Physical Geography, 34(3) 287-326.

Kondolf, G.M. (1994) Geomorphic and environmental effects of instream gravel mining. Landscape and Urban Planning 28, 225-243.

Lane, E. W., (1955) The importance of fluvial morphology in hydraulic engineering. Proceedings, American Society of Civil Engineers, No. 745, July.

Leopold, L.B. and Langbien, W.B. (1962) The concept of entropy in landscape evolution. USGS Professional Paper 500-A, 20 p.

Leopold, L.B. and Maddock, T. (1953) The hydraulic geometry of stream channels and some physiographic implications. USGS Professional Paper 252, 57 p. Washington, DC: US Geological Survey.

Leopold, L.B. and Wolman, M. (1957) River channel patterns: braided, meandering and straight. USGS Professional Paper 282-B. Washington, DC: US Geological Survey.

Mackin, J.H. (1948) Concept of the graded river. Geological Society of America Bulletin, v. 59, no. 5, p. 463-512, doi: 10.1130/0016-7606

Nanson, G. C. (1986) Episodes of vertical accretion and catastrophic stripping: a model of disequilibrium flood-plain development: Geological Society of America Bulletin, v. 97, p. 1467-1475.

Nanson, G. and Croke, J. (1992) A genetic classification of floodplains. Geomorphology 4, 459-486.

Nelson, J. M., and Smith, J. D. (1989) Evolution of erodible channel beds, In: Ikeda, S., and Parker, G. (eds.), River Meandering: AGU Water Resources Monograph 12, Washington, D. C., p. 321-377.

Newson, M.D. and Newson, C.L. (2000) Geomorphology, ecology and river channel habitat; mesoscale approaches to basin scale challenges. Progress in Physical Geography 24, 2, 195-217.

Newson, M.D. and Sear, D.A. (1993) River conservation, river dynamics, river maintenance: contradictions? In White, S., Green, J. and Macklin, M.G. (eds) Conserving our Landscape. Joint Nature Conservancy, Peterborough, pp. 139-146.

Oreskes, N., Shrader-Frechette, K. and Belitz, K. (1994) Verification, validation and confirmation of numerical models in the earth sciences. Science 263, 641–42.

Osterkamp, W. R., and Hupp, C. R. (1984) Geomorphic and vegetative characteristics along three northern Virginia streams: Geological Society of America Bulletin, v.95, p. 1093-1101.

Palmer, M.A., Ambrose, R.F., and Poff, N.L. (1997) Ecological theory and community restoration ecology. Restoration Ecology 5, 291-300.

Petts, G., and Foster, I. (1985) Rivers and Landscape: Edward Arnold, Ltd., London, 274 p.

Phillips, J.D. (2009) Changes, perturbations, and responses in geomorphic systems. Prog. In Phys. Geog. 33(1), 17-30.

Powell, D. (1998) Patterns and processes of sediment sorting in gravel-bed rivers. Progress in Physical Geography 22, 1–32.

Renard, K.G. and Keppel, R.V. (1966) Hydrographs of ephemeral streams in the southwest. American Society of Civil Engineers, Proceedings: Journal of Hydrology Division 92, 33-52.

Richards, K., Brasington, J. and Hughes, F. (2002) Geomorphic dynamics of floodplains: ecological implications and a potential modeling strategy. Freshwater Biology 47, 559-579.

Rust, B.R. (1978) A classification of alluvial systems. In Miall, A.D. (ed.) Fluvial Sedimentology. Canadian Society of Petroleum Geologists. Calgary, Memoir No. 5, pp. 187-198.

Schumm, S.A. (1968) River adjustment to altered hydrologic regimen – Murumbidgee River and paleo-channels, Australia. USGS Professional Paper, 598.

Schumm, S.A. (1969) River metamorphosis. American Society of Civil Engineers, Proceedings; Journal of the Hydraulics Division 95, 255-73.

Schumm, S. A. (1977) The Fluvial System, John Wiley, Hoboken, N. J.

Schumm, S.A. (1985) Patterns of alluvial rivers. Annual Review of Earth and Planetary Sciences 13, 5–27.

Schumm, S.A. (1991) To interpret the earth: Ten ways to be wrong. Cambridge University Press, Cambridge.

Sear, D.A. and Newson M.D. (2010) Fluvial Geomorphology: its basis and methods. In Sear, D.A., Newson, M.D., and Thorne, C.R. (eds) Guidebook of applied fluvial geomorphology. Thomas Telford Limited, London, pp 1-28.

Sheilds, F.D., Jr., Copeland, R.R., Kingman, P.C., Doyle, M.W., and Simon, A. (2003) Design for stream restoration. Journal of Hydraulic Engineering 129(8), 575-584.

Thomsen, B.W. and Schumann, H.H. (1968) Water resourcesof the Sycamore Creek Watershed, Maricopa County, Arizona. USGS Water Supply Paper 1861, 53 pp.

Thorne, C.R. (1998) Stream Reconnaissance Handbook. John Wiley & Sons Ltd., England.

Thorne, C.R., Soar, P., Skinner, K, Sear, D., and Newson, M. (2010) Driving processes II. Investigating, characterizing and managing river sediment dynamics. In Sear, D.A., Newson, M.D., and Thorne, C.R. (eds) Guidebook of applied fluvial geomorphology. Thomas Telford Limited, London, pp 120-195.

USACE (2000). HEC-HMS hydrologic modeling system technical reference manual. Hydrologic Engineering Center, Davis, CA.

van den Berg, J. 1995: Prediction of alluvial channel pattern of perennial rivers. Geomorphology 12, 259– 79.

Vollmer, S. and Kleinhans, M. 2008: Effects of particle exposure, near-bed velocity and pressure fluctuations on incipient motion of particle-size mixtures. In Dohmen-Janssen, C., Hulscher, S., editors, Dohmen- Janssen, C. and Hulscher, S., editors, River, coastal and estuarine morphodynamics (RCEM 2007), London: Taylor and Francis, 541–48.

Webb, R.H., Pringle, P.T., and Rink, G.R. (1987) Debris flows from tributaries of the Colorado River, Grand Canyon National Park, Arizona. USGS Open File Report, 87-118. Washington, DC: US Geological Survey.

Wells, S.G. (1976) A study of surficial processes and geomorphic history of a basin in the sonoran desert, southwestern Arizona. Dissertation, Department of Geology, University of Cincinnati.

Wilson, E.M. (1969) Engineering Hydrology. Macmillan, London.

Wolman, M.G. and Gerson, R. (1978) Relative scales of time and effectiveness of climate in watershed geomorphology. Earth Surface Processes and Landforms 3, 189-208.

Wolman, M. G., and Leopold, L. B., 1957, River floodplains: some observations on their formation: U. S. Geological Survey Professional Paper 282-C, 13 p.

Wright, S. and Parker,G. 2005:Modeling downstreamfining in sand-bed rivers. I: Formulation. Journal of Hydraulic Research 43, 612–19, DOI: 10.1029/2006WR005815.

APPENDIX A:

3D MORPHODYNAMIC INVESTIGATION OF SEDIMENT PLUG FORMATION AND DEVELOPMENT IN THE RIO GRANDE

Submitted to Earth Surface Landforms and Processes

Abstract

A sediment plug is the aggradation of sediment in a river reach that completely blocks the original channel resulting in plug growth upstream by accretion and flooding in surrounding areas. Sediment plugs historically form over relatively short periods, in many cases a matter of weeks. Although sediment plugs are much more common in reach constrictions associated with large woody debris, the mouths of tributaries, and along coastal regions, this investigation focuses on sediment plug formation in an alluvial river. During high flows in the years 1991, 1995, 2005, and 2008, a sediment plug formed in the San Marcial reach of the Middle Rio Grande. Previous studies found weak correlation to plug formation with any historic flow or sediment variables, and identified the need for a detailed study of hydrodynamic and sediment transport processes, associated with plug formation. In 2008 cross section data were collected both prior to and after the sediment plug occurred. Therefore, the 2008 event was used to study the relationships between hydro- and geomorphic variables that led to the development of the sediment plug. Three-dimensional hydrodynamic and sediment modeling was done using Delft3D. Previous studies have sampled sediment transport variables, and along with data collected by USGS, were used to determine sediment transport parameters. Detailed mapping of simulated unsteady three-dimensional hydrodynamic and sediment transport regime, along with channel morphologic change associated with plug formation illustrates linear and non-linear relationships. Results suggest that the presence of cohesive sediment in the water column is required for plug formation and development. Changes to hydraulic and sediment parameters are not proportional to morphologic changes and are asymptotic

in their response. These results suggest the existence of thresholds for plug formation given the conditions of the 2008 sediment plug and that the contribution of specific variables to plug formation is not uniform.

Keywords: sediment plug, avulsion, Delft3D, Rio Grande, alluvial

Introduction

The San Marcial Reach of the Middle Rio Grande in south central New Mexico has been the subject of much study (Burroughs, 2005; TetraTech, 2004; TetraTech, 2010; FWS, 2005; Gorbach, 1992; Mussetter, 2002). This reach is located just upstream of Elephant Butte Reservoir and downstream of the Bosque del Apache National Wildlife Refuge (Figure 1). Man-made impoundments and channel straightening upstream and reservoir levels downstream of the reach have significant impacts on river morphology. A dramatic result of those changes is the formation of a sediment plug. Sediment plugs are areas where the channel becomes completely filled with sediment, forcing floodwater and bedload out into the floodplain (Happ et. al. 1940), the sediment plug then grows upstream by accretion (Shields et. al. 2000).

The development of a sediment plug in this vicinity has several adverse impacts such as: (1) threatening non-engineered levees on the west side of the river either by erosion or piping, (2) causing a permanent avulsion of the currently perched channel to the east or west of its present location, (3) increasing evaporation and flow conveyance losses and

thus adversely affecting water deliveries to Elephant Butte Reservoir, (4) and destabilizing or loss of existing native plant communities and other habitats, including wetlands that are connected to the shallow groundwater table (Tetra Tech 2010). These threats motivated very detailed investigations of hydrologic, sedimentological, and morphometric characteristics and trends. Empirical relations were used to identify site-specific factors associated with plug development including: (1) a constricted channel, (2) loss of flow to overbanks, (3) low channel slopes, (4) low channel capacity, (5) long duration snow melt flows, (6) non-uniform vertical sediment profile, and (7) highly mobile bed material (Tetra Tech, 2010; Buroughs, 2005, Buroughs, 2007). However, these same conditions occurred when sediment plug development did not. Based on the results of both of these studies, prediction of future plug development both spatially and temporally is of limited resolution due to the stochastic nature of the hydrology and local changes in channel and floodplain morphology over time (Tetra Tech 2010).

In developing the Sediment Plugs in Alluvial Rivers (SPAR) model, Burroughs (2005, 2007) identified five independent variables that can be used to predict plug formation. Tetra Tech (2010) found three primary (1°). and three secondary (2°) variables (Table 1). The difficulty with the implementation of SPAR is that the required input data are difficult to determine and monitor, SPAR does not account for river planform morphodynamics, and should not be used when flows exceed the 5-yr annual return period flow rate. The conundrum we are left with in assessing the Tetra Tech (2010)

analysis is that sediment plugs do not occur under similar reach conditions as those identified.

Table 1. Comparison of independent variables associated with plug prediction.

Buroughs (2005)	Tetra Tech (2010)
Flow lost to overbank area as a fraction of the inflow to the reach	1°. Channel width (~39.6 m)
The number of days that flows are lost to overbank areas.	1°. Lack of main channel hydraulic capacity (~56.6 m^3/s)
Ratio of sediment load to initial main channel cross section area.	1°. Perching of the channel above the surrounding floodplain (1.5 to 3 m)
Total sediment load power function exponent.	2°. Presence of bends
	2°.Highly variable channel width
	2°. Presence of clay layer on the bed of the channel.

This study attempts to augment these studies and shed light on sediment plug formation and development through implementation of a three dimensional morphodynamic model to examine hydraulic and sedimentological parameters and investigate possible threshold conditions.

The morphodynamic processes that facilitate the formation and development of sediment plugs in alluvial rivers are very complex, poorly understood, and very few observations exist. It is therefore not possible to build a fully calibrated and validated predictive model for the sediment plug phenomenon. Nevertheless, models can be applied to determine the relative importance of some of the processes and parameters which can be better understood, through numerical experiments (van Maren, et. al., 2009). The objective of

this paper is to analyze the erosion and depositional processes during sediment plug formation and development, using observations and numerical experiment, and explore hydraulic and geomorphic thresholds associated with the phenomenon.

Sediment Plug Formation

There is very little empirical evidence of how sediment plug formation proceeds, as existence of the plug is alerted only after it has formed. However, Burroughs (2007) summarized his findings from Burroughs (2005) stating sediment plug formation is associated with, "a continued, abrupt, significant and permanent loss of flow from the main channel of an alluvial river with high sediment concentrations, accelerated deposition ensues due to the disproportionate loss of flow to the loss of total sediment load." Burroughs (2005) attributes this discrepancy to the vertical distribution of the suspended sediment concentration. Our three-dimensional model allowed us to test this hypothesis.

Sediment plug formation is due to localized disequilibrium between sediment supply and transport capacity. Rivers typically respond to this disequilibrium through a combination of channel widening and aggradation resulting in slope increase (Schumm, 1977). Sediment plugs may form over relatively short periods, in many cases a matter of weeks (Diehl, 2000). Although sediment plugs are much more common in reach constrictions associated with large woody debris, the mouths of tributaries, and along coastal regions,

this investigation focuses on sediment plug formation due to excessive sediment load in alluvial rivers.

The two efforts to unlock the mystery of how and why this sediment plug occurs differ in their assumptions about how the plug forms. As quoted above, Burroughs (2007) believes that a significant loss of flow from the main channel, an avulsion, coupled with a more sediment laden flow left in the main channel results in plug formation. The work of Tetra Tech (2010) assumes that plug formation is due to crossing an aggradational critical threshold. Detailed three-dimensional mapping of bed elevation change sheds light on the process of plug formation.

Stream Stability and Avulsion

Sediment plug formation and channel avulsion are inextricably linked. Much interest in channel avulsion has resulted in a significant body of work which attempts to identify those conditions that determine their frequency and location (Slingerland and Smith, 1998; Jones and Schumm, 1999; Jerolmack and Paola, 2007; Mohrig et. al., 2000; Jerolmack and Mohrig, 2007; Ashworth et. al., 2007). Researchers have identified several threshold conditions for avulsion that we tested in our effort to apply this theory to the San Marcial sediment plug and determine the formation process.

Avulsion is the relatively rapid shift of a river to a new channel on a lower part of a floodplain, alluvial plain delta or alluvial fan (Allen, 1965). In braided streams, the term

avulsion may be used to describe the shift of the main thread of current to the other side of a mid-channel bar (Leedy et. al., 1993: Miall, 1996), we restrict our definition to a complete shift of the entire channel. Avulsion is distinguished from lateral migration, the other primary method of channel relocation, which involves the gradual erosion and removal of bank sediments and their deposition downstream. Avulsion occurs when an event, usually a flood, of sufficient magnitude and/or duration occurs along a reach of a river that is at or near an avulsion threshold. The closer a system is to the threshold, the smaller the event needed to trigger the avulsion (Jones and Schumm, 1999; Schumm, 1977). Proximity to the avulsion threshold explains why avulsions are not always triggered by the largest floods on a given river (Brizga and Finlayson, 1990; Ethridge et. al., 1999).

There is a strong association between channel aggradation, the subsequent perching of the main channel above the floodplain, and channel avulsion (Slingerland and Smith, 2004). Channels become susceptible to avulsion once they super-elevate themselves, via differential deposition. Based on statistical sampling of the paleologic record, Mohrig et. al. (2000), found channel avulsion occurs in a condition in which the channel top is approximately one channel-depth above the surrounding floodplain. This finding suggests that avulsion may be characterized as a threshold phenomenon that allows slow storage and rapid release of sediment within a fluvial system (Jerolmack and Paola, 2007). Our three-dimensional model allows us to test this proposed threshold condition based on the updated morphologic grid after each simulation time-step.

Jones and Schumm (1999) identify four groups of causes for channel avulsion, shown in Table 2, based on an increase in the ratio of the slope of the potential avulsion course (S_a) versus the slope of the existing course (S_e). Decreases in S_e, associated with group 1, and reduction of sediment transport capacity may result in clogging. Avulsions in the second group result from prolonged aggradation of channel and levees resulting in the ratio S_a/S_e to be as high as 30 (Elliot, 1932). Although elevation of the thalweg above the channel floodplain is not necessary in order to reach the avulsion threshold (Schumm et. al., 1996), avulsions in group 2 are less likely to result in channel clogging. Group 3 includes events such as channel-blocking mass movement, possibly associated with sediment inputs from ephemeral streams. Group 4 is a catch all for avulsions that cannot be explained by the first three groups. Table 2 indicates that only sediment influx from tributaries can both trigger an avulsion and result in a decrease in sediment transport capacity.

Table 2. Causes of avulsion (Jones and Schumm, 1999)

Processes and events that create instability and lead toward an avulsion threshold, and/or act as avulsion triggers		Can act as a trigger?	Ability of channel to carry sediment and discharge.
Group 1. Avulsion owing from increase in ratio, S_a/S_e[*], owing to decrease in S_e	a. Sinuosity increase (meandering)	No	Decrease
	b. Base level fall (decrease slope[ψ])	No	Decrease
Group 2. Avulsion owing from increase in ratio, S_a/S_e, owing to increase in S_a	a. Natural levee/alluvial ridge growth	No	No Change
	b. Alluvial fan or delta growth (convexity)	No	No Change
Group 3. Avulsion with no	a. Hydrologic change in flood	Yes	Decrease

change in ratio, S_a/S_e	peak discharge	Yes	
	b. Sediment influx from tributaries, increased sediment load, mass failure,		Decrease
	Aeolian processes		Decrease
	c. vegetative blockage		Decrease
	d. Log or ice jams		
Group 4. Other avulsions	a. Animal trails	No	No Change
	b. Capture (diversion into adjacent drainage	-	No Change

* S_a is the slope of the potential avulsion course, S_e is the slope of the existing channel.
ψ In setting where the up-river gradient is greater that the gradient of the lake floor or shelf slope, base level fall may result in river flow across an area of lower gradient.

Channel avulsion theory proposes several possible threshold conditions for channel avulsion. Not all of the theories suggest the resulting clogging of the channel; however, stream stability and the proximity to the avulsion threshold conditions proposed is a testable metric given the three-dimensional morphodynamic model implemented.

San Marcial Reach of the Middle Rio Grande

During high flows in the years 1991, 1995, 2005, and 2008, a sediment plug formed in the San Marcial reach of the Middle Rio Grande. The Bureau of Reclamation has spent millions of dollars dredging the channel to restore flows to Elephant Butte Reservoir. The 1991, 1995, and 2005 events all occurred at a geologic constriction in the river and are associated with high water levels in the Elephant Butte Reservoir. Conversely, the 2008 event is not associated with high reservoir level or a geologic constriction. In 2008 cross section data was collected both prior to and after the sediment plug occurred. Therefore, the 2008 event was used to study the relationships between hydro- and geomorphic variables that led to the development of the sediment plug.

Channel morphologic changes along the study reach are largely the result of flow regulation at Cochiti Dam, diversions to the Low Flow Conveyance Channel from 1959 to 1985, backwater effects of Elephant Butte Reservoir, and the constriction at the San Marcial railroad bridge (MEI, 2002). The net result of these changes are: (1) a narrowing of the channel from 606.5m in 1918 to 58m in 2008, (2) an increase of 57% in the incoming sediment load to the reach from upstream, and (3) a continual bed level rise of approximately 8m since 1917 (Tetra Tech, 2010). Bed level rise between 2002 and 2005, prior to that plug formation, was up to 1.2m.

The sediment transport capacity to sediment load imbalance in the lower part of the San Acacia reach is severe, channel banks are erosion resistant due to dense vegetation and cohesion (Gray and Leiser, 1989; Smith, 1976), resulting in increased aggradation of the channel bed and its levees. The Middle Rio Grande has one of the highest sediment loads of any river in the world, with measured sediment concentrations as high as 200,000 ppm (mg/l), but the average annual concentrations are reported to have fallen from 24,000 ppm in the 1950s to about 5,000 ppm at present (Baird, 1998). Nordin and Beverage (1964) found that temporary storage of fine sediments on islands and point bars become sources of sediment during sustained high flow events.

A monthly analysis of total sediment load in this reach found that it is not in phase with the annual hydrograph (MEI, 2002). The total sediment load at the San Marcial Bridge is

highest during August, long after the high flows are passed in the spring. This phase lag is attributed to additional sediment inputs from ephemeral streams during summer monsoon season storm events. Tributary derived sediments are of silt and clay size classes and may form a cohesive mud layer. Erosion of this layer is more time-dependent than shear dependent, and therefore, may remain buried during winter flows. Spring snow-melt flows are incapable of breaching the mud layer, resulting in more flow forced out of the banks. In 2009, early season flows over-topped banks at less than 25.5 m^3/s, followed by an abrupt 0.15m drop in river stage with no accompanying drop in flow rate (Tetra Tech, 2010).

Observations

Another reason we used the 2008 sediment plug occurrence is the presence of pre- and post-plug geometric data. In February of 2008, at low flow, the USBR collected cross section data along this reach of the Middle Rio Grande. The sediment plug was first noted (it may have formed earlier) on May 17, 2008. The USBR returned to the site of the plug and noted the cross sections that were filled with sediment (Figure 2). Although no new cross section surveys were conducted, the extent of the plug was noted on those surveys previously measured. The USBR provided this research effort with a one-dimensional HEC-RAS model that contained cross section data compiled from those surveys conducted before and after the sediment plug occurred and other cross section data collected during 2002, 2006 and 2007, which extended upstream to the HWY380 Bridge.

The USGS maintains several stream gauges along the Middle Rio Grande. The nearest upstream gauge is located above US HWY 380 near San Antonio, NM, approximately 11 miles upstream of the 2008 sediment plug. The San Marcial railroad bridge is also gauged and is located approximately 1.3 miles downstream of the end of the plugged portion of the reach.

Sediment transport data was collected by the USGS at the San Marcial Bridge on numerous occasions between 1990 and 1996 (USGS, 1988-2003). Samplers used to collect suspended sediment samples include the DH-48, DH-59, and DH-74. The total sediment supply curve used in this study was derived by Burrough (2005) from 67 data points for the total sediment load computed with data collected at random times between 1990 and 1996 at San Marcial Bridge.

$$Total\ Load\ (tons/day) = 1.4074 \times Flow(cfs)^{1.2419} \quad (1)$$

Studies by MEI (2002) used the entire post-Cochiti Dam historical record to derive suspended and bed material rating curves. Figure 3 illustrates that Burroughs (2005) function results in more than both of those curves but less than the sum of the two MEI (2002) curves. This discrepancy is counter intuitive due to the above average flows that occurred in both 1991 and 1995 that are included in Burroughs' (2005) curve. The discrepancy may be accounted for by significant variability in the historic record most likely the result of temporary storage of fine materials that are later flushed downstream during rising or higher flows (Nordin and Beverage, 1964)

The construction of Cochiti Dam has had a significant impact on the grain material size. Grain size coarsening is most significant immediately downstream of the dam and becomes less pronounced with distance from the dam. In the study reach little coarsening has occurred. Median grain size (D50) approximation was found to be 0.26mm (MEI, 2002).

Modeling

Model Description

In this study we use the state-of-the-art 'sediment online' version of the Delft3D-FLOW model to simulate planform morphologic change. Delft3D solves the unsteady shallow water equations in two- and three- dimensions under the hydrostatic pressure assumption and computes sediment transport and morphologic update simultaneously with flow; see Lesser et. al. (2004) for a description and validation. At each time-step, morphologic updating is based upon the change in bed material that has occurred as a result of the sediment sink and source terms and transport gradients. The change in mass is then translated into a bed level change based on the dry bed densities of the various sediment fractions. Delft3D has been applied previously to reproduce the effect of high sediment concentrations on channel patterns of sediment laden rivers (van Maren, 2007; van Maren et. al., 2009).

Transport of suspended sediment is calculated by solving the three-dimensional advection diffusion equation for suspended sediment. Cohesive sediment exchange with the bed is

computed based on the Partheniades-Krone formulations (Partheniades, 1965). The Partheniades-Krone formulation distinguishes erosion and deposition rates based on the ratio of shear stress (τ) to critical shear stress (τ_c), hindered fall velocity (w_s), average sediment concentration near the bottom computational layer (c). Three input parameters include critical shear stresses for both erosion ($\tau_{cr,e}$) and deposition ($\tau_{cr,d}$), along with a user defined erosion parameter (*M*) that reduces the quantity of erosion calculated by a factor less than one.

$$Erosion = M\left(\frac{\tau}{\tau_{cr,e}} - 1\right) \text{ for } \tau > \tau_{cr,e}\ Erosion = 0 \text{ for } \tau < \tau_{cr,e} \quad (2)$$

$$Deposition = w_s c\left(1 - \frac{\tau}{\tau_{cr,d}}\right) \text{ for } \tau < \tau_{cr,d}\ Deposition = 0 \text{ for } \tau > \tau_{cr,d} \quad (3)$$

Non-cohesive sediment erosion and deposition is determined by the van Rijn (1993) method. The van Rijn (1993) method determines settling velocity based upon D50, the density of the sediment fraction, and the kinematic viscosity. Deposition and erosion fluxes are computed at each half time-step due to upward diffusion from the reference level and downward sediment settling. The sink term is solved implicitly in the advection diffusion equation, whereas the source term is solved explicitly. Van Rijn's reference height controls the suspended sediment concentration gradient in the vertical profile through the standard Rouse formulation. A user defined proportionality factor permits the user to control vertical concentration gradient and the reference level at which

concentration is zero. However, the reference height is limited to a maximum of 20% of the water depth.

Model Application

A fundamental problem with modeling the sediment plug phenomenon on the Middle Rio Grande is the absence of high resolution bathymetric and hydrodynamic data. Bathymetry is needed to build the model, and hydrodynamic (water levels, flow velocity, and sediment concentration) data is needed to calibrate the model. Dramatic changes occurred to the bathymetry of the study reach and we have only the locations of beginning and end of where the main channel is plugged and no data related to where and when channel avulsions occurred. Due to the computational intensity of the three dimensional model, the model domain was limited to the approximately five mile stretch that was plugged, an additional mile upstream and approximately two miles downstream to capture the effects of the San Marcial Bridge.

The computational grid was constructed by converting station/elevation cross section points along with right, left, and main channel distances between cross sections into xyz points. A computational grid (M=256, N=51, K=10) could then be built based on these points. Lateral grid distance was minimized in the main channel in order to capture small bathymetric changes and main channel levee top elevations (Figure 4). Vertical grid spacing included 10 layers, where bottom layers were more closely spaced than those near the water surface (Figure 5).

Upstream flow boundary conditions were determined using data from the stream gauge at HWY380 along with the HEC-RAS model provided by the USBR, and the flow loss function derived by Burroughs (2005). Mean flow data from 1998 through 2003 at both the San Marcial and San Acacia stream gauges were used to estimate the amount of water lost to seepage and evapotranspiration. The loss function was developed to estimate losses per 500 foot incremental spatial step:

$$\frac{Loss}{500ft}(cfs) = 0.00028XFlow(cfs) + 0.227 \quad (4)$$

The 2008 sediment plug is estimated to have occurred on May 17, 2008. Due to the computational intensity of three dimensional unsteady modeling a window of time was chosen from April 20, 2008 to June 20th, 2008. The flow records from this time window at the HWY380 bridge were used as an upstream boundary condition for the one-dimensional HEC-RAS hydraulic model. The resultant hydrograph from the one-dimensional model was used to first determine the amount of water lost to seepage and evapotranspiration, and based on the distance from the HWY380 to the upstream boundary of the simulated domain, approximately 10.6 miles, the input hydrograph was determined (Figure 6). Based on grid characteristics and the Courant-Frederich-Lewy number, a computational time step of six seconds was used (Courant et. al., 1967). A stage-discharge rating curve was used for the downstream flow boundary condition. This relation was derived with the HEC-RAS based upon the geometry of the final cross section of the simulation domain. A generic hydrograph was generated based on those values in the simulation (Figure 7).

Sediment input boundary conditions were the same for both up- and downstream boundaries. Non-cohesive sediment concentrations were input based on the total load function derived by Buroughs (2005). Cohesive sediment was also input at the model boundaries. In the absence of observed data, the cohesive sediment load input was made equal to the non-cohesive load. The decision to add cohesive sediment to the simulation inputs was determined based on test results that indicated little or no main channel deposition with only non-cohesive sediment.

Thresholds and Conveyance Change

Channel conveyance (K) was used as a metric for estimating change in cross section planform. Channel conveyance is a function of cross section area (A), hydraulic radius (R), and channel roughness represented by Manning n constant (n) (Chaudhry, 2008).

$$K = \frac{1}{n} A R^{2/3} \quad (5)$$

The three dimensional hydrodynamic grid permitted the calculation of conveyance across each lateral grid section. Main channel conveyance was determined using Equation 5 and those grid cross sections located between channel levees at the initial time step. Right and left floodplain conveyance was also calculated. Main channel conveyance is then determined at each time step and compared to its initial value in order to determine degree of channel plugging.

The avulsion threshold groups identified by Jones and Schumm (1999) are the function of the downstream and cross-stream slopes. Downstream slope (S_e) was determined by the central difference of the thalweg along the entire computational domain. Cross stream slopes for the right and left floodplain were determined by finding the lowest point on the floodplain (z_{fp}) and subtracting that value from the main channel levee top elevation (z_{levee}) to find the floodplain height (h_{fp}). The cross stream or avulsion slope (S_a) value was found by dividing the horizontal distance from the levee top to the lowest floodplain elevation point (Δx) by h_{fp} (Figure 8). The ratio S_a/S_e could then by tracked across the domain and though time.

The avulsion threshold articulated by Jerolmack and Paola (2007) is a function of the height of the main channel (h_{mc}) and the height of the floodplain as it relates to the height of the main channel levees (h_{fp}). The ratio h_{mc}/ h_{fp} could be determined and tracked down the length of the main channel simulated and at each time step (Figure 8).

Numerical Experiments

Several hydro- and morphodynamic factors were identified by Buroughs (2005) and MEI (2010). This three dimensional model could be used to test all of those variables; however, we focused our efforts on those identified as primary, including the suspended sediment concentration distribution in the water column and the possible role of cohesive sediments in suspension. Suspended sediment vertical distributions at the upstream

boundary were varied to reflect both a uniform, and linearly distributed from zero at the water surface to the maximum at bed level.

Absent more observed data on any cohesive sediment, it was determined that values for the critical shear stress for erosion and deposition would be equal (van Maren et. al., 2009). This decision is also based on findings that small changes in these parameters have little impact on bathymetric updating (van Maren et. al., 2009). Based on a D50 value of 0.26mm (MEI, 2002) and the Shields diagram, a value of 0.18 N/m^2 was used. The erosion parameter (M in equation 2) was varied by orders of magnitude in order to determine the importance of this parameter, and its impact on the morphodynamic bed and main channel bank top elevation changes.

The modeling procedure is as follows: first, the effect of roughness was used to calibrate hydrodynamics based on observed discharge measurements at the San Marcial Bridge; secondly, cohesive sediment is added to the water column as this was found to possibly play an important role in plug formation; thirdly, the erosion parameter (M) was varied to determine the degree to which this parameter affects the timing and extent of plug formation; fourthly, the vertical distribution of suspended sediment was changed from uniform to linearly distributed in order to test the importance of this variable. Many other model tests and runs were implemented, including some of those previously mentioned. Model results reported will focus on those found to be most relevant to plug formation

and development, critical avulsion threshold values, and possible variables that can be measured by personnel in order to predict future sediment plugs.

Model Results

Roughness

Both one dimensional and a two dimensional FLO-2D hydraulic models were built to represent the Middle Rio Grande (Tetra Tech, 2010). During the design phase of the Low Flow Conveyance Channel a Manning n-value of 0.017 was used for the main channel of the entire San Marcial reach (USBR, 2000). Channel roughness coefficients in the FLO-2D model ranged from 0.016 in the plane-bed reaches near the Bosque del Apache wildlife refuge to 0.06- for the large riprap below the diversion dams (Riada, 2007). Floodplain Manning's n-value coefficients used by Riada (2007) changed from 0.080 to 0.120. Calibrated values found by Tetra Tech (2010) ranged between 0.016 and 0.032 in the main channel and overbank n-value coefficients ranged from 0.060 to 0.090. The overall reduction in roughness coefficient can be explained by the reduction in channel conveyance capacity between 2005 and 2009.

The impact of roughness on the downstream hydrograph (Figure 9) shows that higher roughness values result in higher peaks and lower troughs. Concurrent with these findings, a comparison of Figures 10a and 10b illustrate that lower roughness values result in more channel scour in reach constrictions, and more variability in main channel conveyance change. Further testing not included in figures confirmed the increase in

scour with smaller roughness coefficients. Due to our interest in representing aggradation and the small difference in response hydrograph, further simulations were done with n-values at the high end of the scale.

Cohesive Sediment

The presence of cohesive sediment in the water column has a dramatic effect on channel morphodynamics. Figure 11a illustrates how conveyance changes over time for cross sections 177 through 181. These sections represent the length of reach just upstream of the small radius of curvature left bend, and are identified as the location most likely for sediment plug formation. Figure 11a shows that while conveyance increases throughout the inflow hydrograph, some deposition does occur during the rising limb of the biggest peak flow rate.

A dramatic difference in conveyance can be seen in Figure 11b that illustrates the impact of non-cohesive sediment in the simulation domain at those same cross sections. A reduction in conveyance of the main channel happens almost immediately and continues to decline during most of the simulation. Figure 11b elaborates on the timing and spatial distribution of main channel aggradation, by illustrating that conveyance loss occurs first at the downstream cross section. This conveyance loss then travels upstream by accretion, evidenced by the reduction occurring later in time with decreasing m-index. Channel conveyance reduction illustrated in Figure 11b is not correlated to any particular flow

rate, but is connected to the sharp bend and reduced stream width that occurs near cross section m=190.

In order to confirm the role of cohesive sediment and test the correlation to flow rate, Figures 12a and 12b are histograms of the frequency of occurrence of the minimum channel conveyance for ten groups of dates (corresponding flow rates are found on Figures 13 and 14). Figure 12a illustrates that given only sand size sediment fractions approximately 70 percent of the cross section's minimum channel conveyance occurs at the beginning of the simulation, or conveyance increases during the simulation time period. By contrast, Figure 12b shows that more cross sections reach their minimum value at the end of the simulation than the beginning and that more cross section's conveyance is minimized during the simulation time period corresponding to peak flows. Due to the results of these findings, cohesive sediments were included in further model simulations.

Erosion and sedimentation settings

As stated previously, the authors had no justification for setting the erosion and deposition critical shear stresses as two different values, which corresponds to the findings by van Maren et. al. (2009). Nevertheless, van Maren et. al. (2009) found that the erosion parameter setting (M in equation 2) did have a significant impact on results. Initial cohesive sediment runs were completed with M=1.0E-3 $kg/m^2/s$. Figure 13 illustrates the change in main channel conveyance from the initial to the minimum value

for model simulations with both M=1.0E-3 and 1.0E-5 kg/m^2/s. The two solutions are similar, with the exception of two notable areas, those sections from m=32 to m=64 and m=161 to m=178. Model behavior is consistent in both areas with the lower erosion coefficient resulting in scouring upstream before a rapid drop in channel conveyance. The lower erosions parameter results in decreasing main channel conveyance across the domain with some small exceptions; however, the magnitude of conveyance loss is similar with both erosion parameter values. Further simulation were competed with M=1.0E-5.

Testing was also done on the vertical distribution of suspended sediment due to the importance of this parameter found by Burroughs (2005). Delft3D has sediment boundary condition settings that include the vertical distribution of suspended sediment including uniform, linear, step, and layer specified. Testing was done with uniform and linear vertical suspended sediment distributions. Results showed that a linear distribution of zero at the water surface and a maximum value near the bed has almost no impact on conveyance change. Testing was also done with reference density for hindered settling (c_g) parameter. A c_g of 1600 kg/m^3 is typical for sand suspension; however, during more fine grained floods, c_g is probably closer to 300 kg/m^3 which results in hindered settling, especially in floodplains (van Maren et. al., 2009). Testing results with a reduced c_g value do not significantly impact main channel conveyance changes.

Morphometrics and Channel Avulsion

Channel width is clearly an important factor in controlling sediment transport capacity. Channel contraction increases depth creating a backwater effect that reduces transport capacity upstream of the constriction (Sturm, 2000). Figure 14a shows clearly that there are three channel constrictions in the domain located at approximately m=50, 100, and 200. Channel constrictions appear to be correlated to significant reductions in main channel conveyance. Previous works on this phenomenon also cited the importance of channel constriction; however, this is not a predictive variable due to the multiple channel constrictions where sediment transport capacity is sufficient for sediment load (Burroughs, 2005; Tetra Tech, 2010)

Previous works on this phenomenon also cited the importance of channel width. However, their focus was exclusively on the width of the main channel and not floodplain width, as reported above (Burroughs, 2005; Tetra Tech, 2010). Figure 14b illustrates both main channel conveyance and width, and suggests that there is no direct relation. These authors agree with previous works in determining that channel width is not a predictive variable due to the multiple channel constrictions along the Middle Rio Grande where sediment transport capacity is sufficient for sediment load and sediment plugs do not occur (Burroughs, 2005; Tetra Tech, 2010).

Model simulation results show that channel avulsion did occur along with formation of the sediment plug. Figure 15 illustrates the difference between initial and final bed elevations. These results show that the main channel was plugged through most of the

domain. The results also show that a new main channel did develop in the right side floodplain through the middle of the simulation domain and on the left side floodplain upstream of the low radius bend. Channel avulsion threshold metrics were tested on simulated bathymetric changes. The ratios of lateral and downstream slopes (Sa/Se) for both right and left floodplains were determined. Figure 16 shows the results of the slope stability analysis. There are three distinct areas of the domain that have relatively large slope stability ratios, representing potential avulsion slopes being much greater than the downstream slope. A comparison with main channel conveyance change suggests that slope stability ratio is highly correlated with conveyance change, as each area of high slope stability ratios are followed by decreases in channel conveyance.

In order to test the avulsion threshold theory put forth by Jerolmack and Paola (2007), a height stability threshold was defined as the ratio of floodplain depth (h_{fp}, Figure 8) to main channel depth (h_{mc}). Larger values represent more dramatic perching of the floodplain. Figure 17 shows the height threshold ratio for both right and left floodplains, as well as channel conveyance change. The results in Figure 17 are similarly correlated as the slope stability ratio (Figure 16) with the exception of the drop in conveyance associated with the low radius bend at approximately m-index=180. A ratio above one does occur in the vicinity, larger values do not. Significant channel aggradation and perching is seen in many cross sections. Figure 18 illustrates that cross sections associated with significant main channel conveyance loss, such as cross sections m=80

and m=160, experience significant channel aggradation and perching prior to formation of the sediment plug.

In order to understand the relationship between main channel conveyance loss and channel avulsion several representative cross sections were analyzed. Figure 15 illustrates that several avulsions occurred in the simulated length of reach; however, a new avulsion channel carrying the main flow does not form down the entire reach. There are several areas where flow passes across the floodplains. Where avulsions do occur, Figure 19 suggests that main channel conveyance loss occurs simultaneously with formation of a new channel. It also shows that as channel aggradation occurs, levees are over-topped and main channel height decreases.

Discussion

The aim of this paper was to analyze the morphodynamic processes in a small section of the Middle Rio Grande using both observations and numerical model experiments. These analysis efforts are complicated by (1) the low resolution bathymetric data available, (2) limited bed sediment characteristic sampling, (3) the long distance between stream gauges, and (4) lack of velocity measurements. Nevertheless, the model applied here is able to reproduce some of the morphodynamic processes occurring in this river reach. Given the limited data available, some assumptions had to be made.

The major assumption is that the flow contains sand, silt and clay sized particles. Although there are limited measurements to support this assumption, there are several factors that led to its implementation. First and foremost, model simulations with only sand sized particles resulted in no main channel deposition and in fact led to main channel erosion. In addition, field reconnaissance found evidence of (1) exposed thick clay layers at the lower portion of incised channel banks and in the channel bed, (2) channel incision, narrowing, and the increase in sediment transport capacity is known to have occurred upstream of the simulated reach, and (3) a large number of tributary arroyos are located on the east side of the river and have been mechanically connected to the Rio Grande (Tetra Tech, 2010). Lastly, the possible importance of non-cohesive sediments was identified by both previous studies of this reach (Burroughs, 2005; Tetra Tech, 2010), and emphasized by the latter. One of the six measures identified by Tetra Tech (2010) to prevent or limit future plug formation is the ripping of the channel bed to break up clay layers.

Other assumptions used in this modeling effort include the concentration of cohesive sediment fractions along with the size distribution. We also assumed that the cohesive sediment fraction followed the same flow dependent concentration as the non-cohesive sediment. We also assumed a constant grain size distribution, which is related to the formation of space filling networks and the transition from erosion to deposition and vice versa (van Maren et. al., 2009). Flow calibration of a two dimensional model done in the early 1990's that used velocity measurements at several cross sections found that

Manning's n-values were strongly affected by channel width (FLO, 1995 and 1995a). However, we assumed constant values for main channel and overbank areas.

Despite the limitations of the model and its various deficiencies, a three dimensional numerical model in which a large number of the morphodynamic, sediment, and hydrodynamic processes are included is able to reproduce some basic characteristics of main channel conveyance loss in the Middle Rio Grande.

- In the first phase of the development of the sediment plug, channel aggradation results in significant perching of the main channel caused by differential distribution of deposition favoring channel bed and margins due to armoring by both vegetation and presence of cohesive sediment. Channel aggradation continues due to disequilibrium between sediment transport capacity and load from upstream. This ratio is controlled by both channel area and downstream slope.
- During the second phase, main channel bank overtopping occurs and portions of the bank are washed downstream resulting in a large influx of sediment to the main channel. Lateral shifting of the main channel is common in the Rio Grande. The Rio Grande has shifted from a meandering to a braided river along this section of its length which is consistent with movement of large bedforms and changes to channel geometry (MEI, 2002).

- In the third phase, scour begins to occur in depressions in floodplain areas. This scour appears to be associated with contraction of the floodplain area. Floodplain scour and the development of a new main channel direct increasing proportions of water flux from the existing main channel. This shift of main flow increases available energy to the new channel and reduces available energy in the existing channel resulting in increased deposition. The development of an avulsion channel is the result of extended high flows. Sediment plug formation occurs as the input hydrograph begins to wane. The reduced flow input is directed toward the avulsion channel resulting in very low flows and sediment transport capacity in the main channel, eventually plugging the channel entirely.

There is a general consensus on the role of losses to overbank areas. On the Yalobusha River, the main channel conveyance capacity abruptly drops from 566 m^3/s to 71 m^3/s where a sediment plug formed (Simon and Thomas, 2002). In that case, the portion of the river above where the plug formed had been channelized, as higher flows reached the end of this channelized reach, a large portion of the flow went overbank and was dispersed across the floodplain. A sediment plug also formed along the Guadalupe River in Texas during a 2002 flood event. Flows went overbank and were diverted through a swale on the inside of the bend just above where the plug occurred. The Army Corps of Engineers completed a one dimensional hydraulic analysis that found river flows exceeding 1133 m^3/s go overbank into the constructed swale (Gergens, 2003). When the plug formed along the Guadalupe River, flows peaked at 1892 m^3/s and structures located along the

swale were damaged. Overbank flows are also associated with sediment plug formation in the Hatchie River basin (Diehl, 2000).

Burroughs (2005) stated that a sediment plug will form if a specific series of events occurs. First, the daily total sediment load into the reach should exceed the historical average daily total sediment load. This study finds that total sediment load must also include a significant fraction of non-cohesive sediment size fractions in that load in order for plug formation to occur. Second, a significant portion of the flow abruptly overbanks (within a few thousand feet longitudinally along the river) – the sediment transport capacity is reduced without the same proportional reduction in the sediment load causing deposition to ensue in the main channel. This assertion is consistent with the findings of our study. Lastly, Burroughs (2005) finds that higher flows must be prolonged causing deposition to continue until the main channel is plugged with sediment. This study suggests that higher duration and magnitude flows are required to initiate overtopping of channel banks and channel avulsion to occur; however, main channel plugging occurs as a result of a loss in flow rate that is differentially distributed to the new avulsion channel, resulting in a dramatic loss of original main channel conveyance capacity and the subsequent plugging.

In the present work we show that by implementing these morphologic processes in a numerical model, we can reasonably reproduce the spatial distribution of erosion and sedimentation leading to main channel conveyance loss in a perched channel. However,

this work also demonstrates that the relation between main channel conveyance loss and morphodynamics is even more complex due to the role of bathymetric avulsion thresholds. Furthermore, bathymetric changes and channel avulsion appear to be correlated with a phase lag between events, making predictive correlative relations difficult. Further work will focus on the nature of these correlative relationships. The effect of roughness, stream width, and sediment density on flow velocities and sedimentation/deposition relations, are therefore not instantaneous.

Although this paper shows that we can reasonably reproduce some aspects of main channel conveyance loss using a numerical model, it also demonstrates that we need to study the behavior of channel avulsions in general, and at the receding end of the hydrograph in particular, in more detail.

Conclusions

Main channel conveyance loss, such as that found in the Middle Rio Grande, is hydrodynamically complex and characterized by rapid morphologic changes. Because of the complex nature of this phenomenon it is still poorly understood. A numerical model based on the open source Delft3D flow model reproduces these complex hydrodynamics and morphodynamics reasonably well, in a qualitative sense. From model simulation results and available observations we conclude that:

- Numerical simulations of the hydro- and morphodynamics of the sediment plug phenomenon requires the presence of a cohesive sediment fraction in the suspended and bed sediment loads, that is commonly left out of morphodynamic modeling in alluvial rivers.
- Overbank flow, associated with spring snow melt, results in localized scour in floodplain areas that become conduits for increasing proportions of discharge, reducing the flow rate and sediment transport capacity of the main channel. This interrelationship is cyclic, and eventually the main channel becomes completely plugged.
- Channel avulsion is the cause of plugging of the main channel and not vice versa. Aggradation and perching of the main channel result in increasing ratios of both main channel to floodplain height and the downstream or existing slope to the avulsion or new channel slope. Downstream of those areas that experience high ratios of both of these morphometric variables, significant main channel conveyance is lost. Although slope stability appears to be a better predictor of avulsion, the commensurate loss of main channel depth and increase in floodplain depth occurs in areas where channel perching is not significant.
- The impact of floodplain width on morphodynamics is much greater than the impact of main channel width. Dramatic morphologic changes occur during floodplain flow. Main channel geometry and its relation to the floodplain influence the preferential flow paths of moving water and sediment; however, floodplain geometry and the placement of the main channel in that context is

more highly influential in determining morphologic changes during high flow events.

Acknowledgements

We thank Dr. Vince Tidwell of Sandia National Labs for ideas, assistance, and patience. NSF Award EAR-0846523 is also appreciated for their support of Dr. Jennifer Duan. Support for this research was provided by Sandia National Labs, the Salt River Project, and the staff at Bureau of Reclamation Albuquerque Area Office. We would also like to thank the researchers at Deltares for their technical support (on their community forum) and nurturing of the research community.

Figures

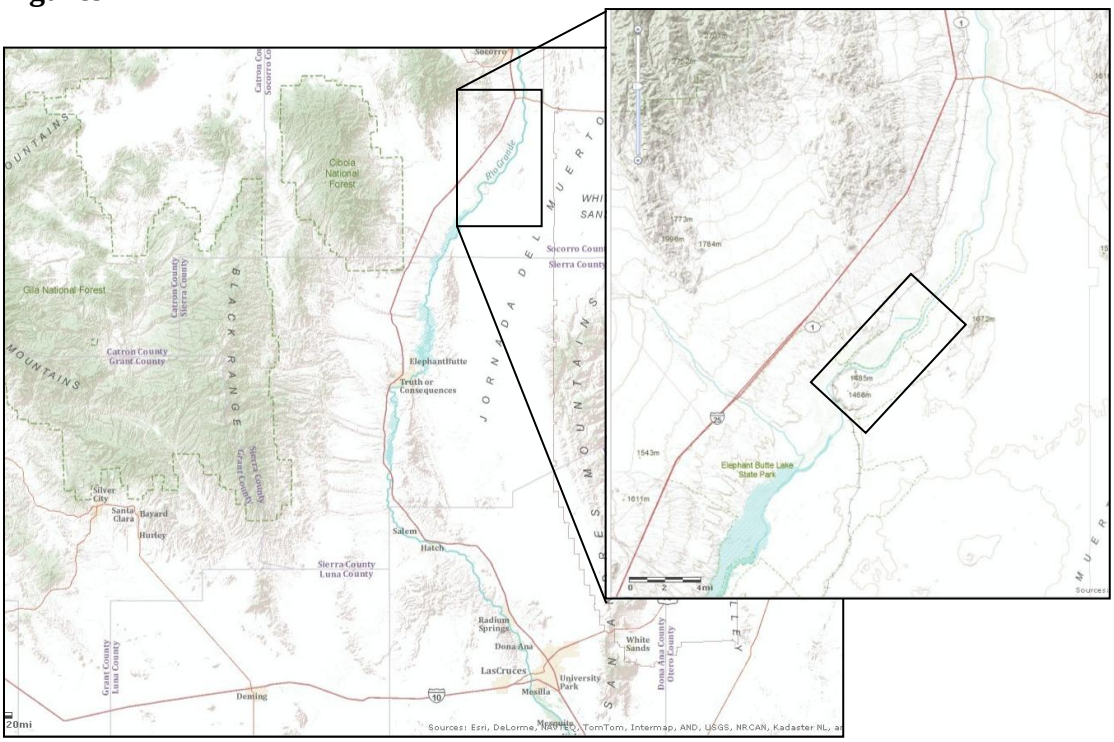

Figure 1. Location Map

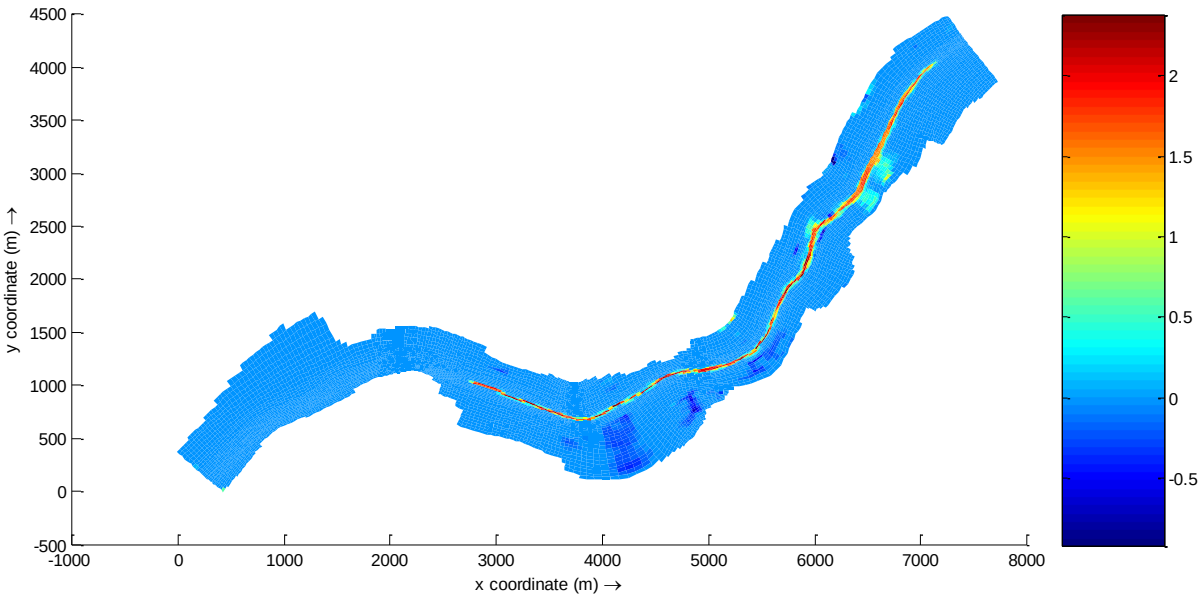

Figure 2. Location of 2008 sediment plug from cross section data provided by USBR.

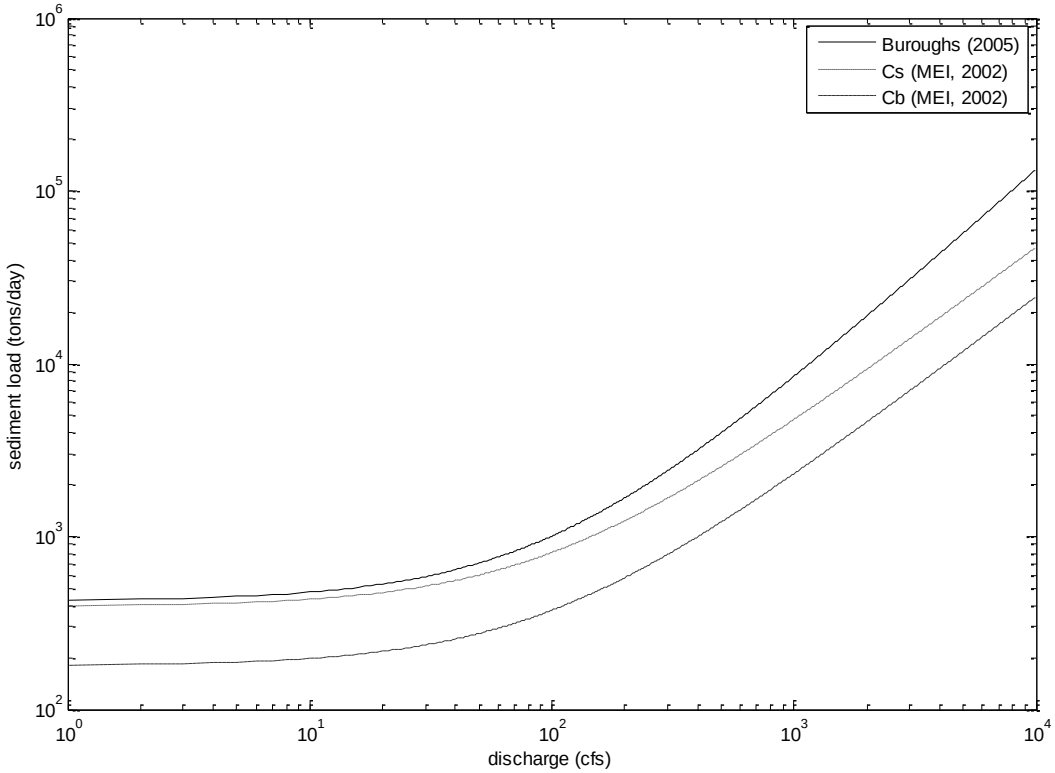

Figure 3. Suspended sediment (Cs) and bed load (Cb) functions for San Marcial derived from (MEI, 2002) along with total load function from Burroughs (2005).

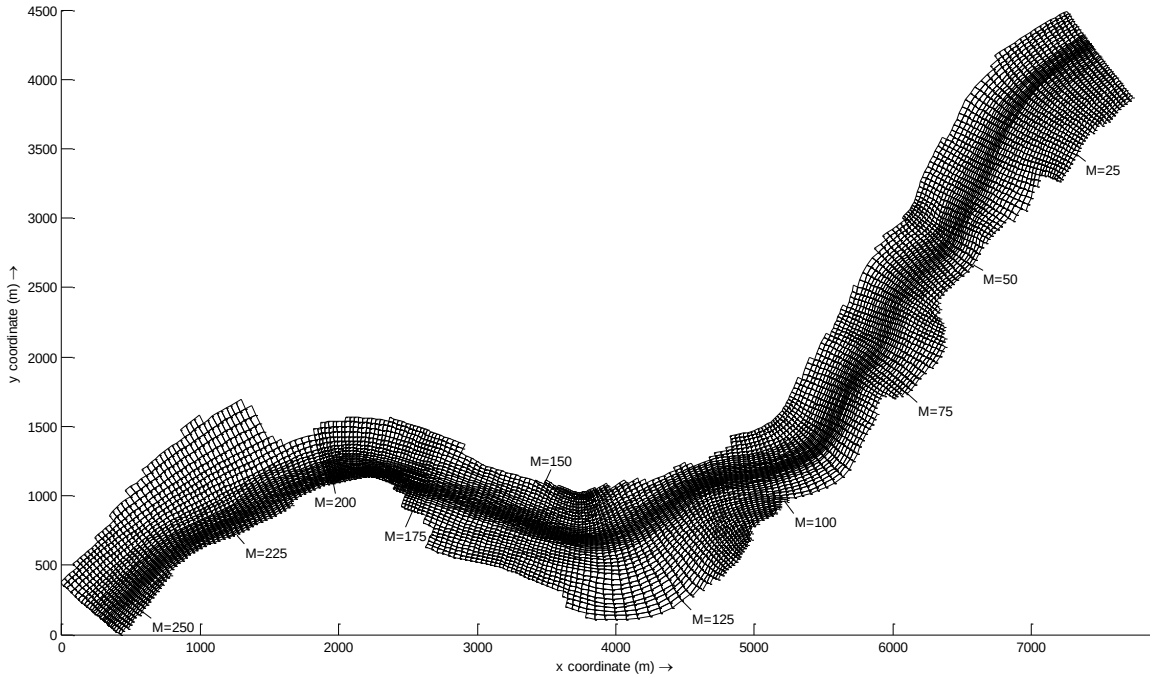

Figure 4. Morphodynamic grid illustrating finer grid resolution in area of main channel and downstream m-index for some reference cross sections.

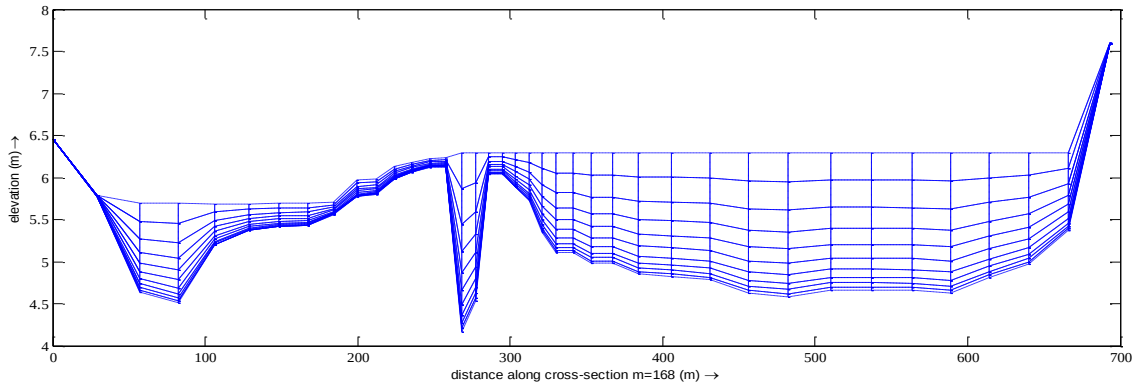

Figure 5. Hydrodynamic grid illustrating non-linear vertical grid distribution.

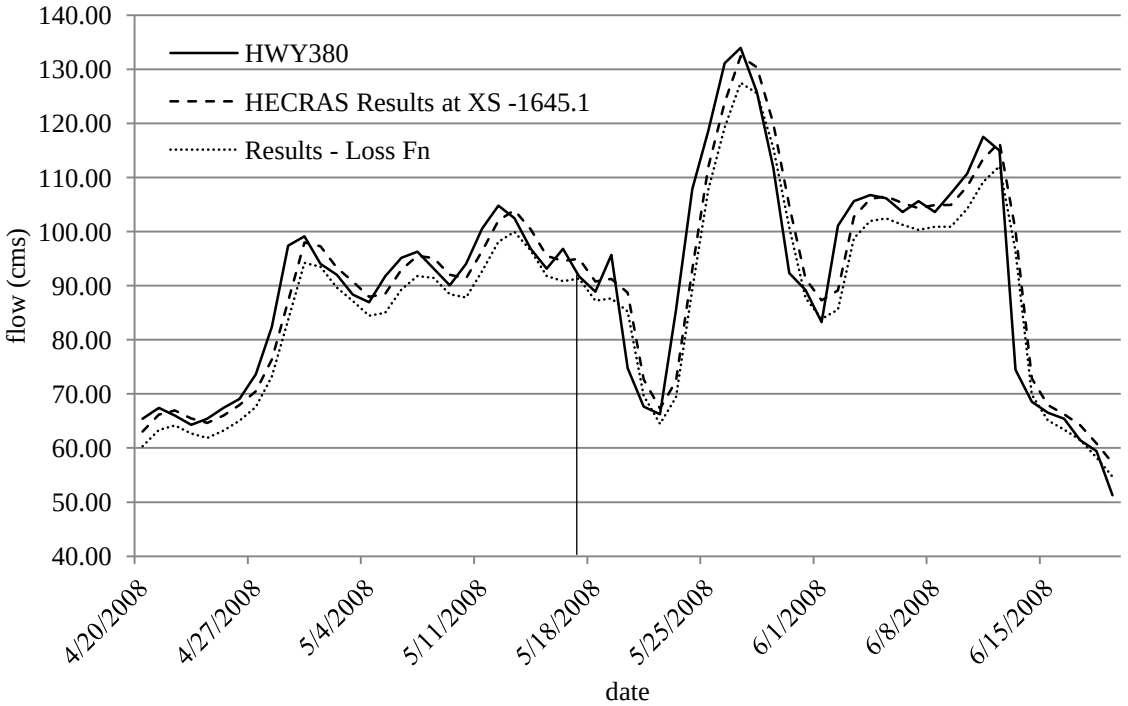

Figure 6. Input hydrograph derivation from observed and simulated data. Line indicates time plug was found.

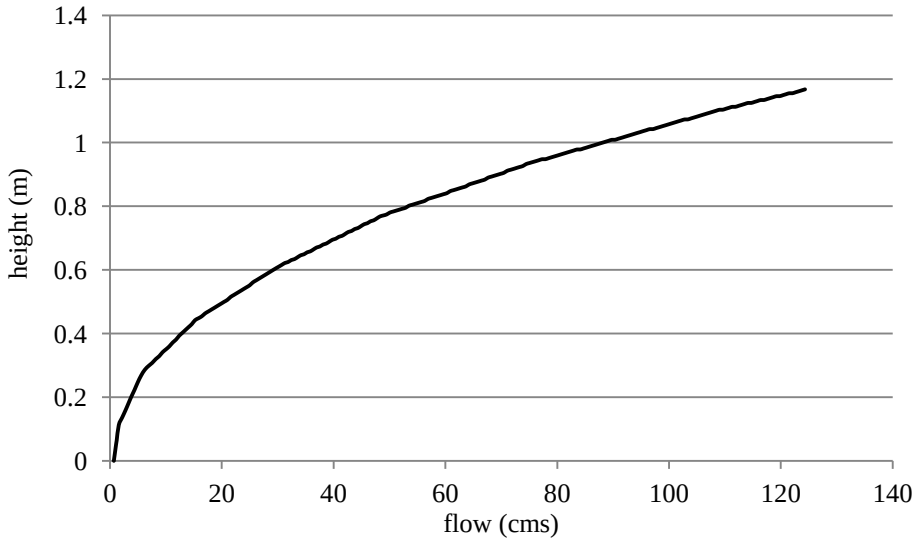

Figure 7. Stage-discharge relation of domain downstream boundary.

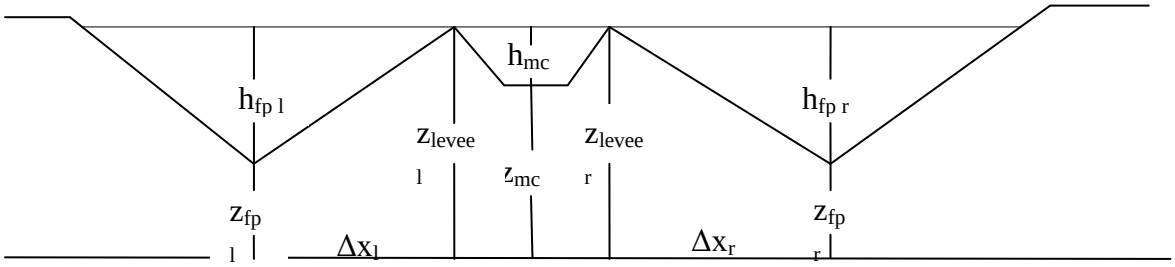

Figure 8. Schematic of cross section geometry related to avulsion threshold stability.

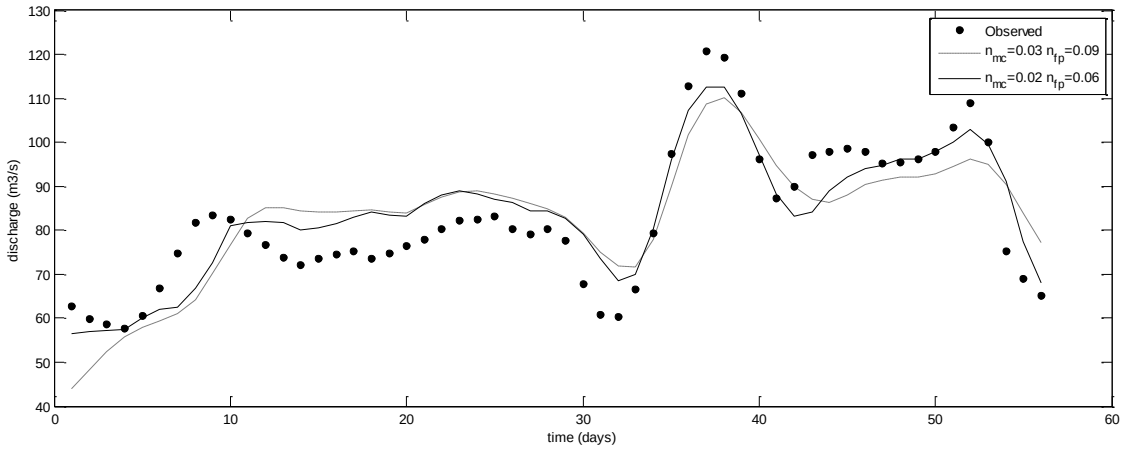

Figure 9. Simulated and observed hydrographs at San Marcial Bridge. Simulations with lower Manning n values captures the peaks and low flow periods more closely than a higher roughness coefficient.

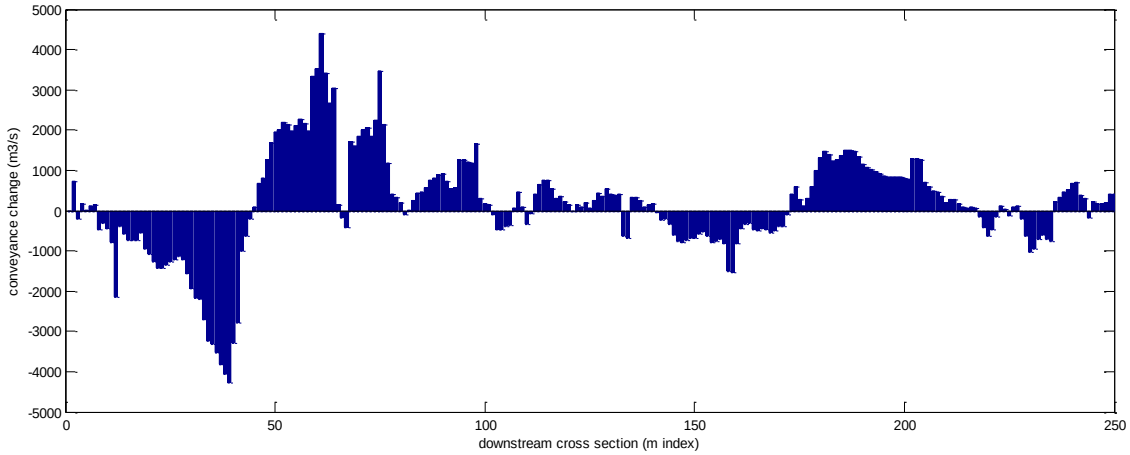

Figure 10a. Simulated conveyance change when n_{mc}=0.03 and n_{fp}=0.09.

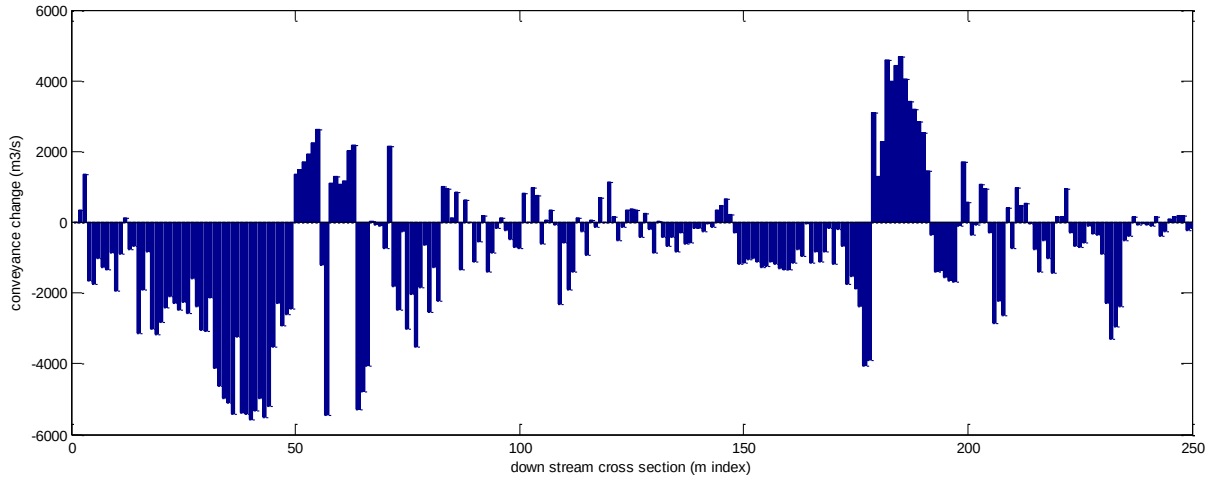

Figure 10b. Simulated conveyance change when n_{mc}=0.02 and n_{fp}=0.06.

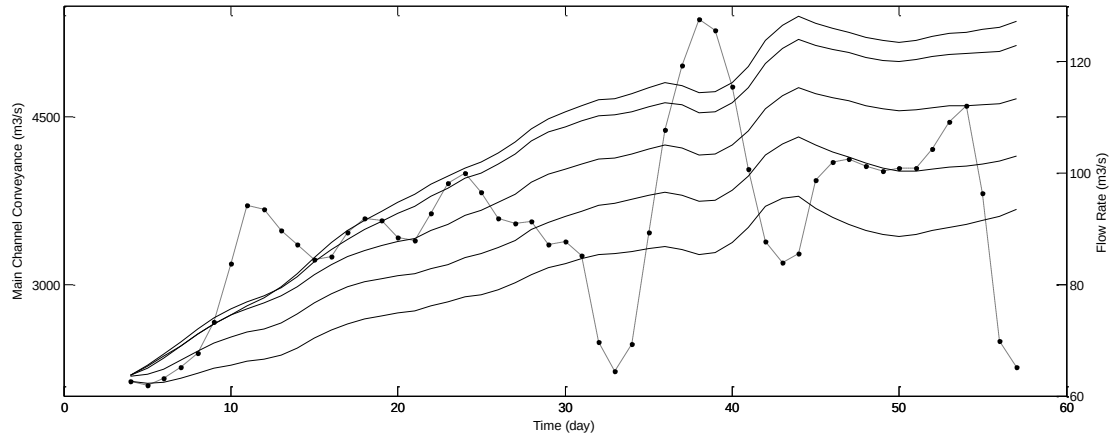

Figure 11a. Simulated main channel conveyance over time for cross sections 177 to 181, representing the length of reach upstream of left bend. Inflow hydrograph is added to visualize relation between parameter and variable. Results from simulation with only non-cohesive sediment.

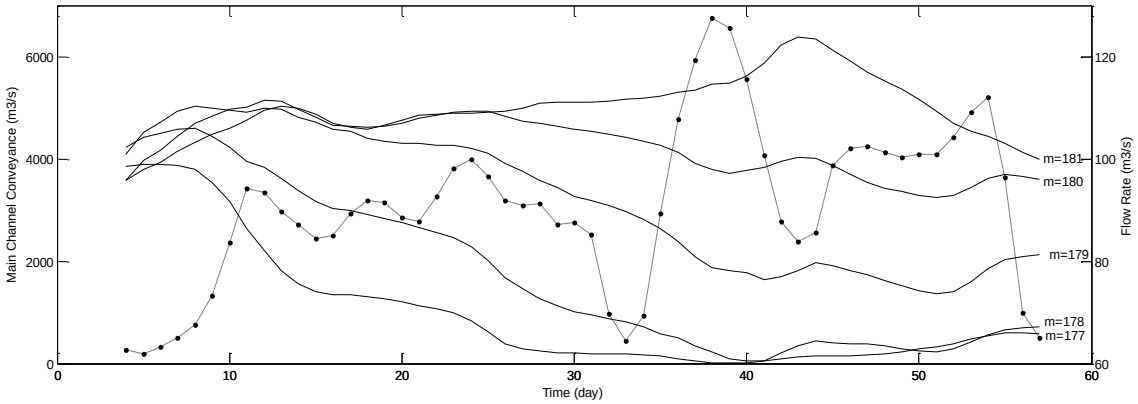

Figure 11b. Simulated main channel conveyance over time for those cross sections listed, representing the length of reach upstream of left bend. Inflow hydrograph is added to visualize relation between parameter and variable. Results are from simulation results with cohesive and non-cohesive sediment fractions (M=1.0E-3).

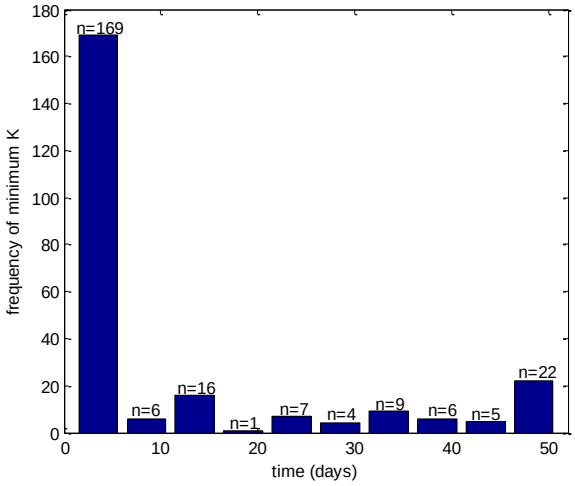

Figure 12a. Histogram of the day, and corresponding flow, that the minimum channel conveyance occurs. Data set from simulation with sand sediment fraction only.

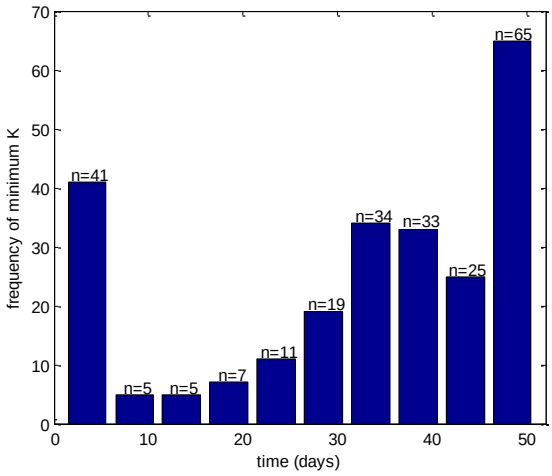

Figure 12b. Histogram of the day, and corresponding flow, that the minimum channel conveyance occurs. Data set from simulation with sand and mud sediment fractions.

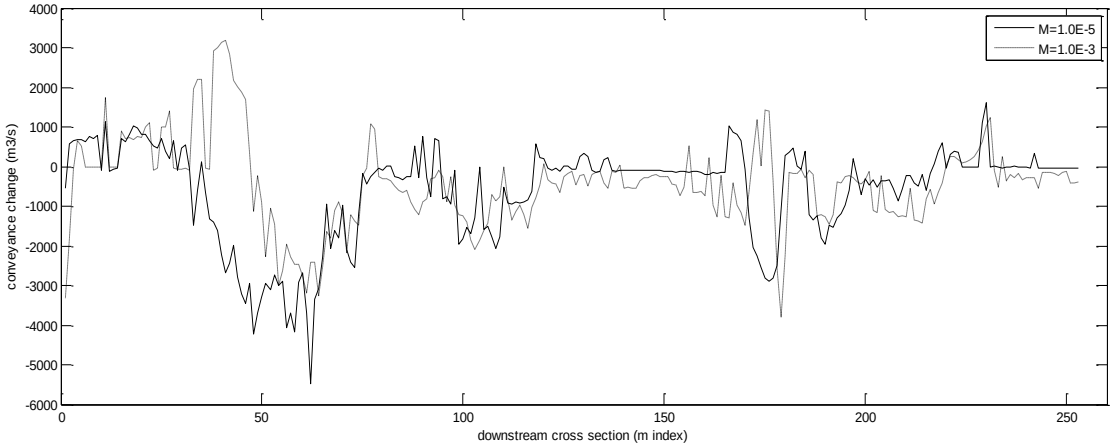

Figure 13. Main channel conveyance change during entire simulation for individual cross sections for M=1.0E-3 and M-1.0E-5.

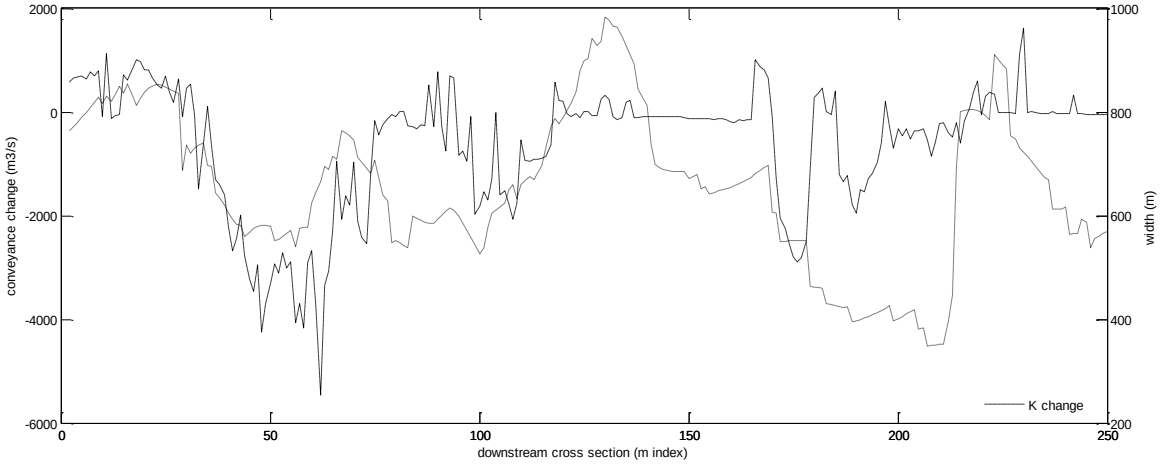

Figure 14a. Stream width and conveyance change.

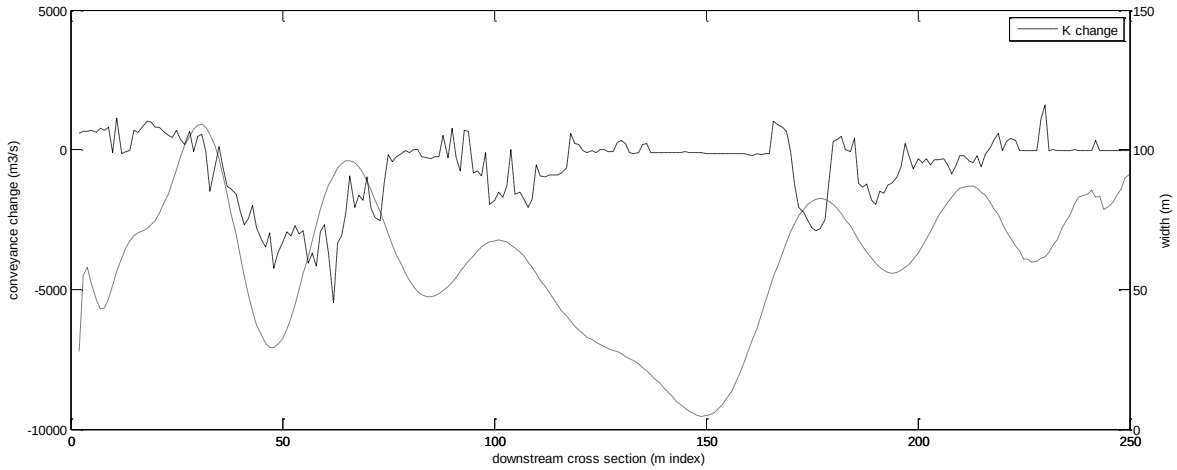

Figure 14b. Main channel width (polynomial fit) and conveyance change.

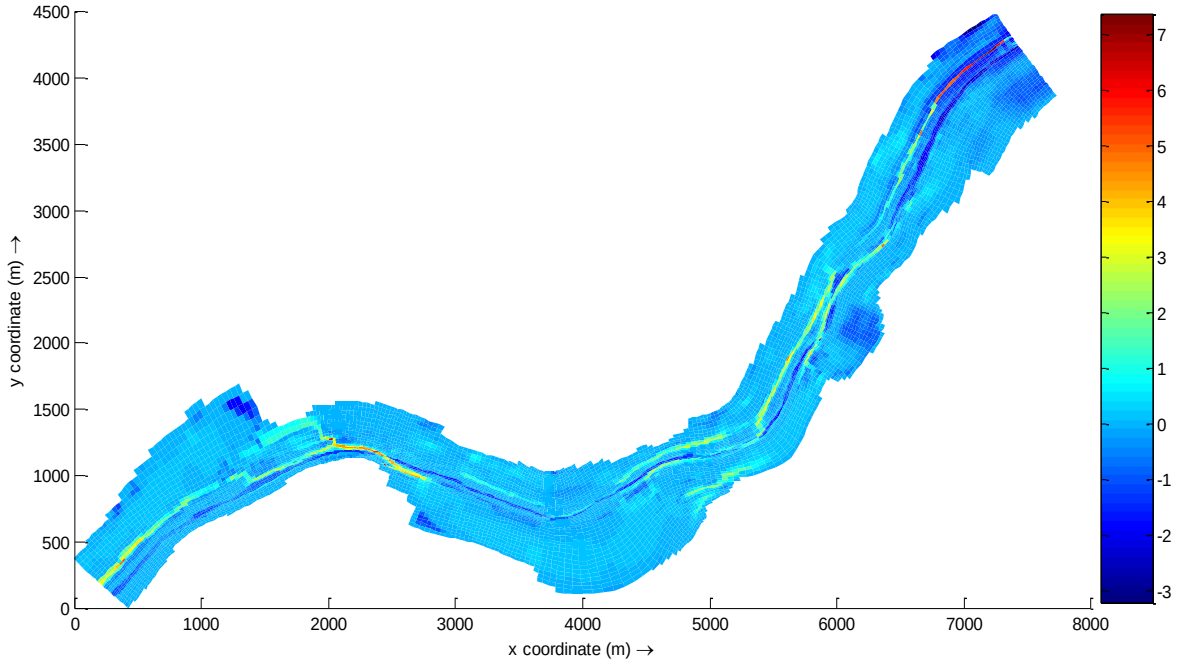

Figure 15. Difference between initial and final bed elevations, where positive values indicate scour areas and negative values indicate deposition.

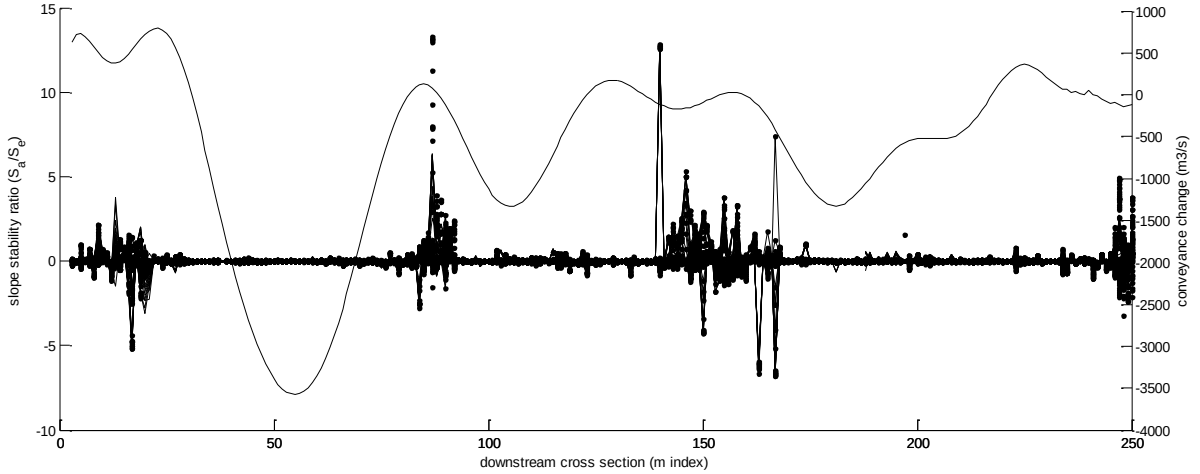

Figure 16. Slope stability ratio for both right and left floodplains on left y-axis and main channel conveyance change (polynomial fit) on the right y-axis.

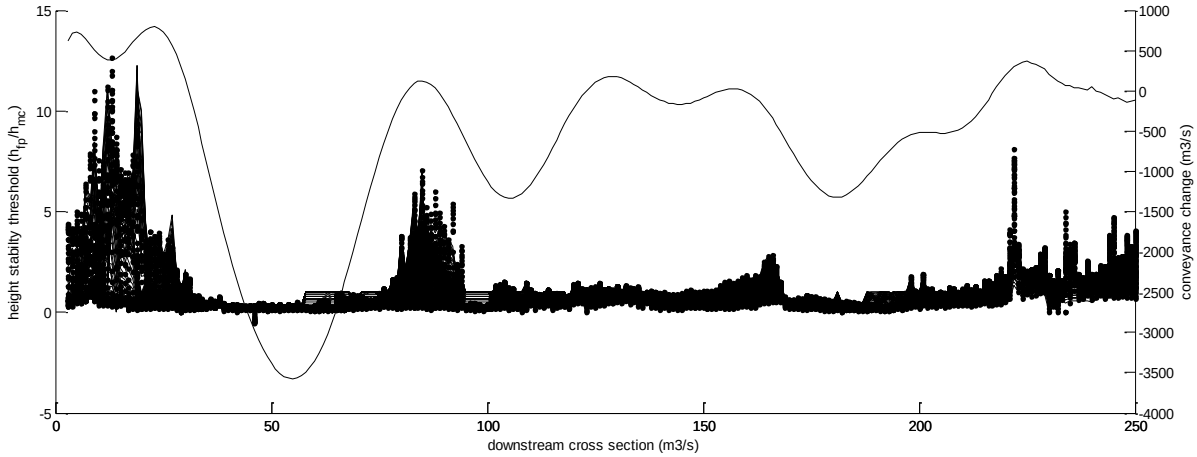

Figure 17. Height stability ratio for both right and left floodplains on left y-axis and main channel conveyance change (polynomial fit) on the right y-axis.

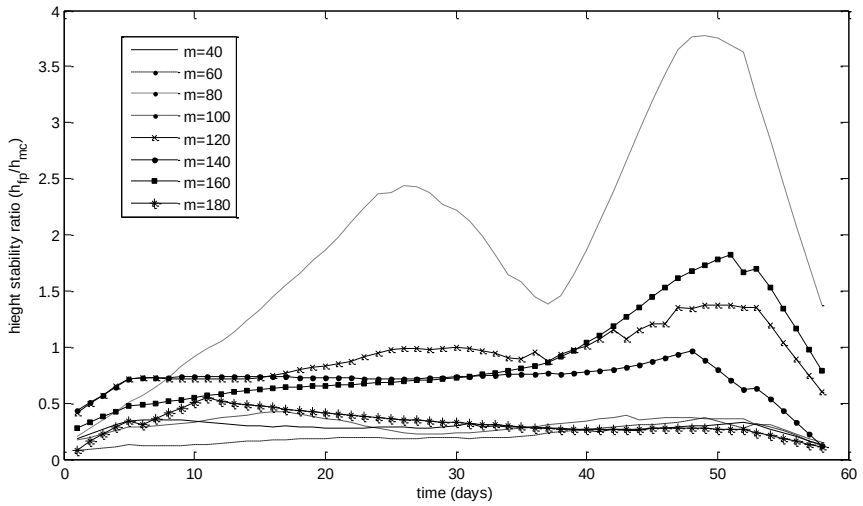

Figure 18. Height stability ratio of several representative cross sections for right floodplain over time.

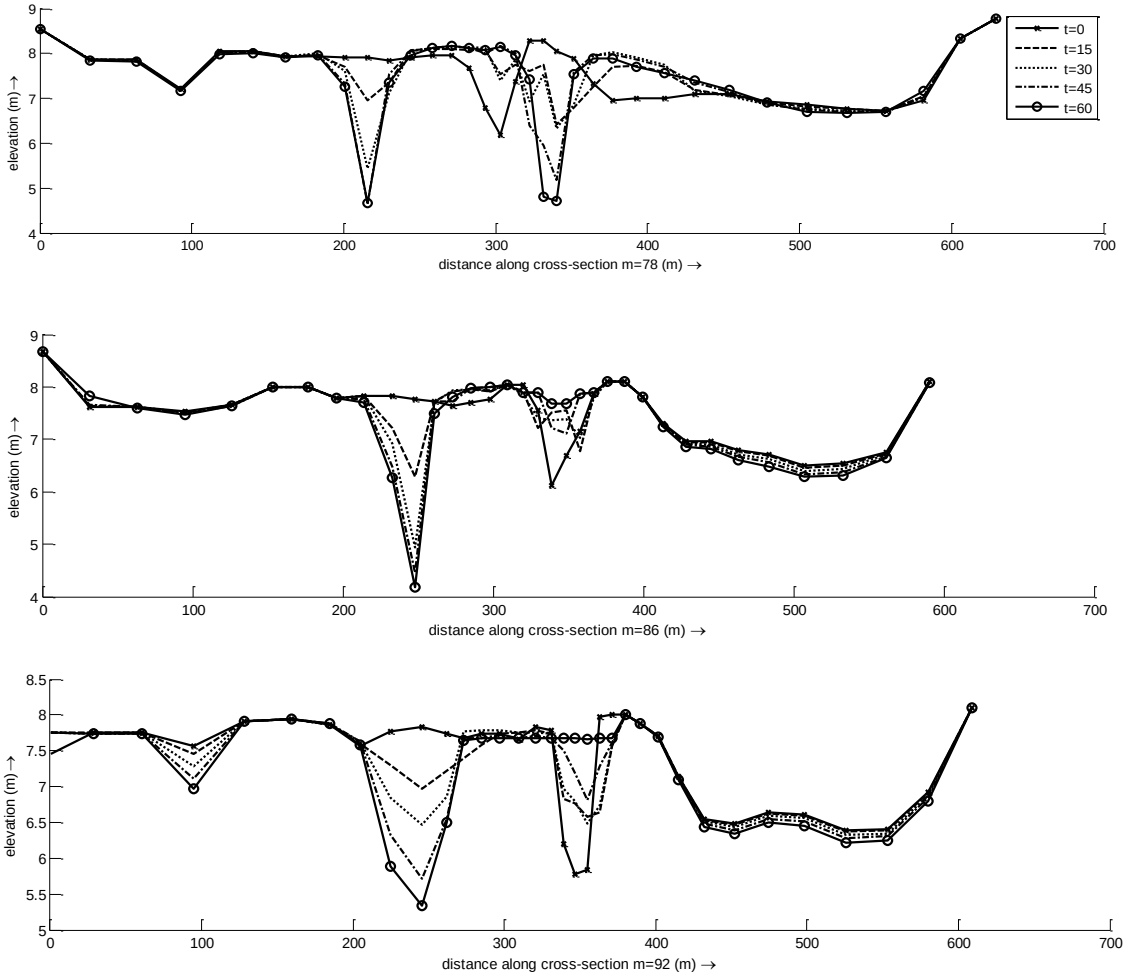

Figure 19. Cross sections upstream of mid-reach constriction, bed elevation changes over time. Initial channel is located at approximately 350 meters and is notably perched above the right side floodplain. Note vertical and horizontal axes at very different scales.

References

Allen, J.R.L. 1965. A review of the origin and characteristics of recent alluvial sediments. Sedimentology, 5, 89-191.

Ashworth, P.J., Best, J.L., and Jones, M.A. 2007. The relationship between channel avulsion, flow occupancy and aggradation in braided rivers: insight from an experimental model. Sedimentology 54, 497-513.

Baird, D.C., 1998. Bank stabilization experience on the Middle Rio Grande. Water Resources Engineering 98, ASCE, New York, NY, p. 387-392.

Brizga, J.S., and Finlayson, B.L. 1990. Channel avulsion and river metamorphosis: the case of the Thompson River, Victoria, Australia. Earth Surf. Process. Landf. 15, 391-404.

Cellino, M. and Graf, W.H. 1999. Sediment-laden flow in open channels under non-capacity and capacity conditions. Journal of Hydraulic Engineering 125(5), 456-562.

Chaudhry, M.H. 2008. Open Channel Flow. Springer Science+Business Media, LLC.

Courant, R., Friedrichs, K., and Lewy, H. (1967) .IBM Journal of Research and Development 11 (2): 215–234.

Diehl, T.H. 2000. Shoals and valley plugs in the Hatchie River watershed. US Geological Survey Water-Resources Investigations Report 00-4279.

Elliot, D.O. (1932) The improvement of the Lower Mississippi River for flood control and navigation, Vol. 1. US Army Corps of Engineers, Waterways experimental Station, Mississippi River Commission, Vicksburg, MS.

Ethridge, F.G., Skelley, R.L., and Bristow, C.S. 1999. Avulsion and crevassing in the sandy, braided Niobrara River, complex response to base level rise and aggradation. In: Fluvial Sedimentology VI (Eds. Smith N.D. and Rogers, J.), Spec. Publs. Int. Ass. Sediment., No. 28 pp 179-191, Blackwell Science, Oxford.

FLO Engineering, Inc. 1995. Manning's n-Value Calibration for SO Lines, 1993 Runoff Season. Prepared for the Bureau of Reclamation

FLO Engineering, Inc. 1995a. Manning's n-Value Calibration for SO Lines, 1994 Runoff Season. Prepared for the Bureau of Reclamation

Gergens, R. 2003. Canyon Lake flood emergency operations. Proceedings from the Watershed System 2003 Conference, May 13-15, Portland, Oregon

Gorback, C.A. 1992. Channel restoration above Elephant Butte Reservoir. Published in Hydraulic Engineering: Saving a Threatened Resource—In Search of Solutions: Proceedings of the Hydraulic Engineering sessions at Water Forum '92. Baltimore, Maryland, August 2–6, 1992. Published by American Society of Civil Engineers.

Gray, D.H. and Leiser, A.T., 1989. Biotechnical slope protection and erosion control. Krieger Pub. Co., Malabar, Florida.

Happ, S., G. Rittenhouse, and G. Dobson. 1940. Some principles of accelerated stream and valley sedimentation. Technical Bulletin 695, US Department of Agriculture, USA.

Jerolmack, D.J., and Mohrig, D. (2007) Conditions for branching in depositional rivers. Geology 35 (5), 463-466.

Jerolmack, D.J., and Paola, C. (2007) Complexity in a cellular model of river avulsion. Geomorphology 91: 259-270.

Jones, L.S., and Schumm, S.A. 1999. Causes of avulsion: an overview. In: Fluvial Sedimentology VI (Eds. Smith N.D. and Rogers, J.), Spec. Publs. Int. Ass. Sediment., No. 28 pp 171-178, Blackwell Science, Oxford.

Leedy, J.O., Ashworth, P.J., and Best, J.L. 1993. Mechanisms of anabranch avulsion with gravel bed braided rivers, observations from a scaled physical model. In: Braided Rivers (Eds. Best, J.L. and Bristow, C.S.) Spec. Publ. geol. Soc. London, No. 75, 119-127. Geological Society of London, Bath.

Lesser, G.R., Roelvink, J.A., van Kestler, J.A.T.M., and Stelling, G.S. 2004. Development and validation of a three dimensional morphological model. Coastal Engineering 51, 883-915.

Miall, A.D. 1996. The geology of fluvial deposits. Springer-Verlag, Berlin.

Mohrig, D.C., Heller, P.L., Paola, C., and Lyons, W.J. (2000) Interpreting avulsion process from ancient alluvial sequences: Guadalope-Matarranya system (northern Spain) and Wasatch Formation, (western Colorado). Geologic Society of American Bulletin 112 (12), 1787-1803.

Musetter Engineering Inc. (2002). Geomorphic and sedimentological investigation of the Middle Rio Grande between Cochiti Dam and Elephant Butte Reservoir. NM Interstate Stream Commission.

Nordin, C.F., and Beverage, J.P.. 1964. Temporary storage of fine sediments in islands and point baras of alluvial channels of the Rio Grande, New Mexico and Texas. US Geological Survey Professional Paper 462-F.

Partheniades, E. 1965. Erosion and deposition of cohesive soils. Journal of Hydraulics Divison, ASCE, 91(HY1), 105-139.

Riada Engineering, Inc. 2007. FLO-2D flood routing model development, Middle Rio Grande Cochiti Dam to Elephant Butte Reservoir, 250 foot grid system. Supplemental Addendum, prepared for the US Army Corps of Engineers, Albuquerque District, January, 21st.

Schumm, S.A. 1977. The Fluvial System. John Wiley and Sons Ltd., NY.

Schumm, S.A., Mosley, M.P., and Weaver. W.E. 1996. Morphology, hydrology, and evolution of the anastomosing Owens and King Rivers, Victoria, Australia. Bull. Geol. Soc. Am. Soc. Civ. Eng. 105, 346-416.

Shields, Jr., F.D., S.S. Knight, and C.M. Cooper. 2000. Cyclic perturbation of lowland river channels and ecological response. Regulated Rivers: Research and Management, 16, 307-325.

Simon, A. and Thomas, R.E. 2002. Processes and forms of an unstable alluvial river system with resistant, cohesive streambeds. Earth Surface Processes and Landforms. 27, 699-718.

Slingerland, R. and Smith N.D. (1998) Necessary conditions for a meandering-river avulsion. Geology 26, 435-438.

Slingerland, R. and Smith N.D. (2004) River avulsions and their deposits. Annual Review of Earth and Planetary Sciences 32: 257-285.

Smith, D.G., 1976, Effect of vegetation on lateral migration of anastomosed channels of a glacial meltwater river. Geological Society of America Bulletin, v. 87, p.857-860.

Sturm, T.W. 2001. Open Channel Hydraulics. McGraw-Hill, NY.

Tetra Tech Inc. 2004. Conceptual restoration plan active floodplain of the Rio Grande San Acacia to San Marcial, NM. Prepared for Save our Bosque Task Force.

Tetra Tech Inc. 2010. River Mile 80 to River Mile 89 geomorphic assessment and hydraulic and sediment-continuity analyses. Prepared for Bureau of Reclamation.

US Bureau of Reclamation (USBR) 2000. Rio Grande and Low Flow Conveyance Channel Modifications, DRAFT Environmental Impact Statement. Albuquerque Area Office, Albuquerque, NM.

US Geological Survey (USGS). 1988-2003. Water Resources Data – New Mexico. Water Year Data Reports prepared by the Water Resources Division. Albuquerque, NM.

US Fish and Wildlife Service (FWS). 2005. Biological opinion on the effects of the Tiffany Sediment Plug Removal. New Mexico Ecological Services Field Office to Bureau of Reclamation.

van Maren, D.S. 2007. Grain size and sediment concentration effects on channel patterns of silt-laden rivers. Sedimentary Geology, 202, 297-316.

van Maren, D.S., and Winterwerp, J.C., Wu, B.S., and Zhou, J.J. (2009) Modelling hyperconcentrated flow in the Yellow River. Earth Surface Processes and Landforms 34, 596-612.

van Rijn, L.C. 1993. Principles of sediment transport in rivers, estuaries, and coastal seas. AQUA Publications, Amsterdam.

APPENDIX B:

SIMULATING RIVER MEANDERING PROCESSES USING STOCHASTIC BANK EROSION COEFFICIENT

Geomorphology (June 2011) doi:10.1016/j.geomorph.2011.05.025

Abstract: This study first compares the first order analytical solutions for flow field by Ikeda et. al. (1981) and Johanesson and Parker (1989b). Ikeda et. al.'s (1981) linear model of bank erosion was implemented to predict the rate of bank erosion in which the bank erosion coefficient is treated as a stochastic variable that varies with physical properties of the bank (e.g. cohesiveness, stratigraphy, vegetation density). The developed model was used to predict the evolution of meandering planforms. Then, the modeling results were analyzed and compared to the observed data. Because the migration of meandering channels consists of downstream translation, lateral expansion, and downstream or upstream rotations, several measures are formulated to determine which of the resulting planform is closest to the experimental measured one. Results from the deterministic model highly depend on the calibrated erosion coefficient. Because field measurements are always limited, the stochastic model yielded more realistic predictions of meandering planform evolutions. Because the coefficient of bank erosion is a random variable, the meandering planform evolution is a stochastic process that can only be accurately predicted by a stochastic model.

Keywords: meander, Monte Carlo, bank erosion, stochastic

1. Introduction

One of the most perplexing and intriguing problems in open channel hydraulics is the phenomenon of river meandering. Motivations for the continued research on a mathematical model to simulate this ubiquitous river planform are to advance our ability to explain complex natural phenomenon, to resolve issues associated with river ecological functions, to protect hydraulic structures such as bridges and levees, to

mitigate erosion and flooding in valuable agricultural and urban lands, to understand the influence of sinuosity on surface/groundwater interaction, and to develop insight into the formation of oil reservoirs created by ancient meandering rivers (Sun, 1996). Research conducted under the Streambank Erosion Control Evaluation and Demonstration Act of 1974 (Sec 32, Public Law 32-251, submitted in December 1981), found that approximately 142,000 bank-miles of streams and waterways are in need of erosion protection. The cost to prevent or control this erosion by means of conventional bank protection methods was estimated to be in excess of $1 billion US annually. The Upper-Mississippi River alone, the cost estimate exceeded $21 million annually.

Simulations of meandering rivers have been reported intensively in literature that includes three major approaches: 1) analytical solutions (Engelund, 1974; Ikeda et.al., 1981; Johannesson and Parker, 1989a, Camporeale et. al., 2007) 2) numerical solutions (Duan, 1998; Duan et. al., 2001a; Darby et. al., 2002) 3) empirical solutions (Langbein and Leopold, 1966). Besides simulating the flow field to solve for flow velocity and shear stress, numerical and analytical models require the estimation of the rate of bank erosion to simulate the evolution of meandering planform from low to high sinuosities. The results of these models, however, are considerably different because of the differences in calculating the rate of bank erosion. Therefore, the goal of this study is to analyze the analytical method of bank erosion and modeling planform evolution by examining the available methods in literature, through developing metrics to measure error in modeling the evolution of meander planforms. The second goal of this effort is to represent this

modeling method through a Monte Carlo simulation whose results we can compare to the usual deterministic representation.

Bank erosion is a natural adjustment mechanism of channels of dynamic equilibrium and non-equilibrium. Alluvial channels adjust themselves to reach regime conditions through the degradation and aggradation of the river bed and also through width adjustment and planform evolution. The rate of bank erosion may depend on a variety of parameters including soil properties, the frequency of freeze-thaw, the stratigraphy of the bank, the type and density of vegetation, and sediment grain size at the toe of the bank (Micheli and Kirchner, 2002, Perucca et. al., 2007). Bank erosion caused by hydraulic forces acting on bank surface and the failure of banks from geotechnical instability of the bank are the most commonly observed bank erosion phenomena in nature. In general, bank erosion of non-cohesive materials usually proceeds through the following sequence: firstly, bed scouring that steepens the side bank; secondly, bank collapse from instability of the scoured bank; thirdly, deposition of the collapsed bank materials at the front of the bank; at last, transportation of the deposited material downstream (Duan, 2005; Darby et al. 2002). The first two stages of the sequence result from fluvial entrainment and geotechnical instability, and the last two stages depend on the sediment transport capacity near the banks. Several mechanisms for mass failure have been observed including planar, rotational, cantilever, or piping or sapping type failures (Osman and Thorne, 1988; Darby and Thorne, 1996). These processes have been of interest to geotechnical engineers with regards to the design of artificial slopes and embankments. Osman and Thorne (1988) developed a theoretical model to calculate the

bank erosion of steep banks of cohesive materials, which researchers modified to include the location and depth of tension cracks (Darby and Thorne 1994), pore-water and hydrostatic confining pressure terms (Darby and Thorne, 1996), soil moisture content, and stochastic property of bank failure (Duan 2005). These solutions require the calibration of soil erodibility index and other parameters, and considerable field data to describe geotechnical properties of the banks. This physically based method has been applied to simulate bank erosion processes of laboratory cases (Darby et. al., 2002; Duan and Julien, 2005), but is limited for long-term simulation of natural rivers because of data constraints. Therefore, this study focuses on the linear bank erosion model (Ikeda et. al., 1981, Camporeale et. al. 2005), a benchmark in modeling meander migration used as reference to compare contemporary efforts.

Regarding the rate of bank erosion, the approach by Ikeda et al. (1981) was among the pioneering works addressing bank erosion when studying alluvial channel processes. In their approach, the rate of bank erosion (ζ), is linearly related to the excess near-bank velocity (u_b'), which is the difference between depth-averaged velocity at the outer bank and cross-sectional mean velocity, through the linear erodibility coefficient (E).

$$\zeta = E u_b' \tag{1}$$

According to Ikeda's equation of linear bank erosion, the bank retreats if the excess near-bank velocity is greater than zero; otherwise, the bank advances. Ikeda et. al.'s (1981) solution to the velocity excess is based on the depth averaged Navier Stokes equations for shallow water flow in curvilinear coordinates, making the traditional

assumptions of steady flow in a constant width channel, with small ratios of width to centerline radius of curvature. Ikeda et. al. (1981) closed the system of equations using the previous analyses (Enguland, 1974; Ikeda, 1975; Kikkawa et.al. 1976; Zimmerman and Kennedy, 1978) where a "scour factor", A, is used to define a relationship between the transverse bed slope and water surface slope. Engelund (1974) suggested a value of 4.0. The theories of Kikkawa et.al. (1976) and Zimmerman and Kennedy (1978) showed that this parameter should increase with the streamwise velocity. Camporeale (2007) showed that the scour factor is a function of the treatment of secondary currents in the formulation of the model. The authors choose to use an average value based on Suga's (1963) analysis of 45 river bends in 10 alluvial rivers in Japan, suggesting a value of 2.89. Using the above assumptions and solving for velocity at the outer bank using the 1st order approximation of Navier Stokes equation in curvilinear coordinate as follows,

$$U\frac{\partial u_b'}{\partial s} + 2\frac{U}{H}C_f u_b' = b\left[-U^2\frac{\partial \mathcal{C}}{\partial s} + C_f\mathcal{C}\left(\frac{U^4}{gH^2} + A\frac{U^2}{H}\right)\right] \qquad (2)$$

where U is the depth-averaged velocity for the stream reach, s is the streamwise distance, H is the reach-averaged depth, C_f is the friction factor, b is the reach averaged half-width, $\mathcal{C}$ is the local curvature, g is the gravitational constant of acceleration, and A is the scour factor. This solution of near-bank excess velocity was then used to predict bank erosion or deposition through the assumption that the rate of bank erosion/deposition is linearly proportional to the near bank velocity, equation 1.

This approach was then used intensively to predict bank erosion (Parker, 1982; Johannesson, 1985) and was foreseen by Hasegawa and Ito (1987). Several authors (Johannesson, 1985), however, corrected the Ikeda et. al. (1981) model when discovering

that it did not account properly for the streamwise pressure gradient. This term gives rise to the irrotational vortex and, thus, results in higher velocities over the inside bank than the outside bank when applied to a developed bend flow over a non-erodible bed that is horizontal in the transverse direction (Johannesson and Parker, 1989b). This result contradicts those findings by Kikkawa (1976), which were also confirmed by the observations of Parker (1982) and Johannesson (1985). As a consequence, when applying the Ikeda et. al. (1981) model, significant calibrations were required to obtain results matching field observations (Johannesson and Parker, 1989b).

Johannesson and Parker (1989b) developed a bend flow model based on the convective transport of primary flow momentum by the secondary flow that results in a significant outward redistribution of primary flow velocity. Although the importance of this phenomenon was recognized by several researchers, the term was neglected by Ikeda et. al. (1981). Whereas a phase shift between the strength of the secondary current and the local centerline channel curvature was identified as an effect of the fluid inertia by Gottlieb (1976) and Kitanidis and Kennedy (1984), it was Ikeda and Nishimura (1986) that retained the fluid inertia in the equation governing secondary flow and included an unverified approximation assuming the phase shift is independent of depth. Johannesson and Parker (1989a) derived a solution to the primary and secondary flows through the use of Engelund's (1974) slip velocity method, a logarithmic velocity profile, and the condition of vanishing shear stress at the water surface. The solution is then generalized for a sinuous channel, where an expansion for small curvature was implemented. By retaining only the linear terms and dropping the second order, $0(\varepsilon^2)$, terms, a solution can

be reached. Through their analysis, Johannesson and Parker (1989a) determined that this methodology, when applied to the solutions developed by Ikeda and Nishimura (1986), yielded velocity distributions that better matched the observed data because of the central assumption that the secondary flow maintains the same vertical profile as of the developed bend flow, with changes only in magnitude and phase. Therefore, the essential contribution of Johannesson and Parker (1989b) can be summarized in the following relation

$$r\frac{du_b'}{d\theta} + 2u_b' = -r\chi_{20}\frac{d\sigma}{d\theta} + (F^2\chi_{20} - 1)\sigma + (A + A_s)\sigma_s \qquad (3)$$

where r is the rescaled wavenumber and is found as the original wavenumber, k, divided by the scaling factor $\epsilon = C_f b/H$, θ is the streamwise downstream angle relative to the x-axis, χ_{20} is the redistribution effect of the secondary flow, σ denotes an order-one dimensionless curvature, A_s is the result of integrating across the stream width the normalized vertically averaged lateral transport of downstream momentum by the secondary flow, σ_s quantifies the strength and the phase shift in the secondary flow because of changing curvature in a sinuous channel and satisfies the relation

$$r\frac{d\sigma_s}{d\phi} + \delta\sigma_s = \delta\sigma \qquad (4)$$

where δ comes from the relation for the secondary flow strength. The final results (Johannesson and Parker, 1989b) can be used as the 1st order analytical solution for the velocity excess in meandering streams of any arbitrary curvature.

The development and analysis of the linear problem of meander morphodynamics was elaborated and articulated by Zolezzi and Seminara (2001) who were able to

distinguish up- and downstream propagation effects including the phenomenon of overdeepening and the importance of a resonant condition that acts as a threshold to distinguish from where meander propagation may occur. The Zolezzi and Seminara (2001) model is the most detailed and encompasses more of the principal morphodynamic mechanisms, in particular a thorough treatment of the secondary flow effects. Because of its complexity and the success of the Ikeda et. al. (1981) and Johannesson and Parker (1989b) models in predicting observed river evolution (Imram et. al., 1999), however, few researchers have adopted the Zolezzi and Seminara (2001) approach. The applicability and constraints of each of the linear perturbation models is given thorough treatment by Camporeale et. al. (2007).

The erosion coefficient is required to account for variations in the properties of bank material, such as cohesion and vegetation. The coefficient for bank erosion, employed by Crosato (1990), included the effect of fluvial erosion and bank failure. The universal coefficient for bank erosion by Hasegawa (1989) relates the rate of bank erosion to the cross-sectional mean velocity, which was validated using data from alluvial channels in Japan. A detailed study of rates of bank migrations and velocity profiles in a southeastern Pennsylvania stream by Pizzuto and Meckelnberg (1989) suggests that the linear equation for bank erosion is suitable for streams with cohesive and relatively uniform bank materials. Hasegawa (1989) used a solution to the sediment continuity equation at a cross-section and found that the rate of meandering migration was a linear function of the velocity excess. Whereas all authors agree that the coefficient of bank erosion is related to geophysical properties of the bank (Hasegawa, 1989; Wallick et. al.,

2006), effects of vegetation (Pizzuto and Meckelenberg, 1989; Micheli et. al., 2004, Perucca et. al., 2007), among other hydrodynamic, planform, and sediment characteristics, only recently have geotechnical properties been tested in an effort to correlate those properties with the linear coefficient of erosion by taking soil samples and submitting them to lab scour tests (Constantine et. al., 2009).

Nearly all studies employing Eq. 1 have used the historical record to calibrate a constant value of the erosion coefficient, E, and then used it to predict future meander propagation (e.g. Larsen and Greco, 2002). Parameters for determining the coefficient of bank erosion, including bank soil properties, channel geometries, and flow fields vary along the stream, and in particular bank soils and bed material, are heterogeneous. A constant coefficient of bank erosion, used for an entire study reach, is inappropriate. All of the parameters along with the random spatial variations in rates of bank erosion led Hooke (1979) and Pizzuto and Meckelnberg (1989) to conclude that a constant value for the coefficient of bank erosion in equation 1 may not adequately represent either systematic or random variations of soil properties, channel geometries, and flow properties that influence the rate of bank erosion. The coefficient of bank erosion should be a stochastic variable with a mean value based on the averaged values of soil, cohesiveness, vegetation density, geometry, and flow properties.

To examine the accuracy of various methods for the simulation of meander evolution, an approach to compare the accuracies of models, must be proposed. River planforms take complex geometries which are best represented in body-fitted curvilinear coordinates. Computer simulation pre- and post-processing involves the conversion from

the curvilinear to the Cartesian coordinates and vice versa. Traditionally errors in models are the differences of the simulated and observed data at discrete time intervals. The field data to verify the results of meandering models are a series of meandering planforms which cannot be assessed by the traditional method. Unique metrics and algorithms must be developed to determine which simulated planform is the best representation of the observed one.

Therefore, the purpose of this study is twofold: first to examine the existing methods for calculating bank erosion and develop a method for quantifying errors of the results from the model and two, to represent the uncertainty associated with the linear coefficient of bank erosion through a Monte Carlo simulation.

2. *Computational Model*

This study developed two one dimensional numerical models for simulating bank erosion and the consequent evolution of the meandering planform. The flow field was based on the 1st order solution of Navier Stokes Equations in the curvilinear coordinate derived by Ikeda et. al. (1981) and Johannesson and Parker (1989b). The Ikeda et. al. (1981) model is based on their solution for velocity excess, u_b'. This model adopts the explicit upstream difference scheme in Eq.4 to integrate Eq.2 (Sun, 1996, Constantine et. al., 2009),

$$\left.\frac{du_b'}{ds}\right|_i = \frac{u_{b_i}' - u_{b_{i-1}}'}{\Delta s} \tag{5}$$

where Δs is the streamwise distance between nodes, subscript i denotes the node number. Boundary conditions include a constant discharge at the inlet and a constant depth of flow at the outlet. The initial conditions are a spatially uniformly distributed erodibility

coefficient, E, and a trapezoidal cross-section. Whereas an analytical solution to equations (2) and (3) exists, the authors found that the numerical solution yielded fewer extraneous results. The recursive equation is written as,

$$u'_{b_i} = \frac{b}{U/\Delta s_i + 2(U/H)C_f}\left[-U^2\frac{\partial \mathcal{C}}{\partial s}\Big|_i + C_f\mathcal{C}_i\left(\frac{U^4}{gH^2} + A\frac{U^2}{H}\right) + \frac{U}{\Delta s_i}\frac{u'_{b_{i-1}}}{b}\right] \quad (6)$$

The variables are defined in Eq.2. The friction factor is an expression of the shear stress, and comes from the solution of the s-momentum equation after a linear perturbation analysis and Taylor expansion to the zero-order, where shear stress is approximated as $\tau_s = \rho C_f U^2$, yielding

$$C_f = gHI/U^2 \quad (7)$$

For an initial sine generated sinuous channel, the downstream angle can be determined by

$$\theta = \theta_0 \cos(ks) \quad (8)$$

where θ_0 is the initial angle, k is the wavenumber defined as $2\pi/\lambda$, where λ is the wavelength, and s is the distance downstream. As the river planform takes an arbitrary form where subsequent nodes may be in any direction, an algorithm using trigonometric identities is required to find the downstream angle. Curvature of the centerline in this model is calculated as the ratio of change in downstream centerline angle with respect to the x-axis over a unit streamwise length.

Linear models have been shown to be very sensitive to the smoothing and re-gridding procedures (Crosato, 2007). The authors used 3-point weighted average smoothing technique, where the two neighboring points were given a one percent weight. Crosato (2007) found that optimal distance between successive grid points was on the

order of a half channel width. To accomplish this, the authors set the initial amount of computation nodes to this threshold and then nodes are linearly interpolated between points after each time step where the downstream distance between successive grid points is greater than the threshold of half the channel width.

Johannesson and Parker (1989b) made some significant changes to the model proposed by Ikeda et. al. (1981). In this model, the analytical solution found to Eq.3 was used with the substitutions suggested, $\phi = ks$ and $r = kH/C_f b^2$, setting initial conditions to zero, and estimating $\sigma_s = \sigma = \mathcal{C}b$ which gives,

$$u_b' = -\chi_{20}\mathcal{C}b + \frac{C_f b^2}{H}\left[\chi_{20}\left(\frac{U^2}{gH}+2\right)-1\right]e^{-\frac{-2C_f b^2 s}{H}}\int_0^s \mathcal{C}(s')e^{-\frac{2C_f b^2 s}{H}}ds' +$$

$$\frac{C_f b^2}{H}(A+A_s)e^{-\frac{-2C_f b^2 s}{H}}\int_0^s \mathcal{C}(s')e^{-\frac{2C_f b^2 s}{H}}ds' \qquad (9)$$

where r is the rescaled wavenumber and is found as the original wavenumber, k, divided by the scaling factor $\epsilon = C_f b/H$, θ is the streamwise downstream angle relative to the x-axis, χ_{20} is the redistribution effect of the secondary flow represented as

$$\chi_{20} = \frac{1}{\chi_1^3}\left(\chi^3 + \chi^2 + \frac{2}{5}\chi + \frac{2}{35}\right) \qquad (10)$$

where $\chi = \chi_1 - \frac{1}{3}$, and $\chi_1 = \frac{0.077}{\sqrt{C_f}}$, σ denotes an order-one dimensionless curvature and can be approximated as $\sigma = \mathcal{C}$b, A_s is the result of integrating across the stream width the normalized vertically averaged lateral transport of downstream momentum by the secondary flow yielding the relation

$$A_s = 181\left(\frac{H}{b}\right)^2\frac{1}{\chi_1}\left(2\chi^2 + \frac{4}{5}\chi + \frac{1}{15}\right) \qquad (11)$$

which is of the same order as the scour factor, A.

This study used the Ikeda et. al. (1981) and Johannesson and Parker (1989b) solutions for the excess velocity, then Eq. 1 was used for solving the rate of bank erosion with an assumption of either a constant or a stochastic erosion coefficient .

2.1 Parameters in Evaluating Modeling Results

To determine which of the resulting meandering planforms most match the experimental measurements, two approaches were used. First, as illustrated in Figure 1, the symmetrical nature of the experimental data permitted the identification of each bend based on its intersections with the x-axis. Each channel planform consists of several bends that are located either above or below the x-axis. Each bend is represented with a series of nodes along its centerline. These nodes of given x- and y-values could then be used to determine several geometric characteristics of the bend, which are the maximum y-value for measuring the maximum lateral extension of the bend, average y-value for the averaged lateral extension of the bend, the standard deviation, and skew of each bend for its upstream/downstream rotation (see Table 3). The standard deviation of y-values over each bend quantifies the sharpness/roundness of the bend. The smaller the standard deviation, the sharper the bend is. The skew of a series of values is the third statistical moment and measures whether the variable is weighted to one side or the other relative to the mean value. Because of the asymmetry of river bends, the skew is one measure to quantify the degree of rotation of the meander bend. These bend characteristics permit a quantitative approach to determine the similarity of simulated and measured bends. For two individual bends, the closer these parameters are, the closer the channel centerlines are. A similar approach was formulated by Frascati and Lanzoni (2009).

Second, the overall error in the model was also determined by comparing the Mean Squared Error along the entire stream line. Because of the complex geometries and coordinate conversions, it was found that a comparison of y-values at specific points along the stream was the most feasible to determine errors in the model. A linear interpolation between nodes found in orthogonal coordinates was used to find y-values at the points of observed data. Figure 2 illustrates the planform evolution of one meander bend at discrete time intervals. The vertical line is used for reference to show the distribution of computational nodes before and after interpolation. Differences between the observed and simulated data can then be determined based on the differences of y-values at the same location.

2.2 Monte Carlo Simulation

The coefficient of bank erosion is treated as a stochastic variable. Based on the systematic study performed by Crosato et. al. (2007) it was found that the coefficient of bank erosion is a bulk parameter that encompasses many sources of error in the model. In this investigation the coefficient of bank erodibility was spatially uniform, but varied with each model iteration. Spatial uniformity is consistent with the experimental results used in the validation of the model. The authors believe, however, that because of the complexities in the mechanism of bank erosion along with a particular source of model error associated with migration models (Crosato et. al., 2007) the representation of the coefficient of bank erosion as a distribution of values may lend insight to the model schema.

To determine the appropriate range of values, Hasegawa's (1989) solution to the sediment continuity at a representative elementary volume was used. Hasegawa found that bank erosion could be estimated through the product of the velocity excess and a constant term, equivalent to the bank erosion coefficient, as follows

$$\zeta = \frac{3q_{s_0}Ttan(\theta_k)\phi_*}{(1-\lambda)H_0U_0}u_b' \quad (12)$$

where $q_{s_0}$is the average bed load transport, $T = \sqrt{\tau_{*_c}/\mu_s\mu_k\tau_{*_0}}$, where μ_s and μ_k are the static and dynamic Coulomb coefficient respectively, $\theta_k$is the transverse slope, $\phi_* = \tau_{*_0}/\tau_{*_0} - \tau_{*_c}$, λ is the porosity, H_0 is the average depth, and U_0 is the average velocity. In Eq. 14, *T,* and θ_k varied with instantaneous properties of flow turbulence, therefore, are random variables, whereas λ is the porosity and its spatial distribution depends on the local soil moisture content, which is a random variable. Several authors have noted the uncertainty associated the rate of bank erosion (Wallick et. al., 2006; Pizzuto and Meckelnberg, 1989). Wallick et. al. (2006) found that the errors in their estimates of coefficients of bank erosion because of the variations in river planforms to be in the range of ±10% to ±15%. Micheli and Kirchner (2006) used the historical data of the rate of bank erosion and Eq. 1 to back-calculate coefficients of bank erodibility for wet and dry meadows along the south fork of the Kern River. The back-calculated coefficients varied spatially and temporally. Table 1 summarizes the percent error in their estimates. The results showed an average error of approximately 10%. Therefore, based on these field data (Wallick et. al., 2006; Micheli and Kirchner, 2002), the coefficient of bank erosion was determined to vary by about 10% from its mean value at a given river reach. Larger variations are expected in a long river reach of complex geometry, where bank soil

properties are stratified, areas where vegetation may play a large role in streambank migration, and smaller variations are expected for the laboratory experimental channel.

2.3 Distribution of Stochastic Variable, E

To establish what distribution of the stochastic variable to use, a review of each variable in the system was done to help establish a justification for the use of a particular distribution. The instantaneous bed shear stress in Eq. 14 can be either normally or log-normally distributed (Lopez and Garcia, 1999; Cheng and Law, 2003). The Cheng and Law (2003) experimental study indicated that the log-normal distribution converged to a normal distribution when the relative intensity of bed shear stress, denoted as the ratio between the deviation and mean of bed shear stress, is small. In shallow open channel flow, the turbulence intensity is much smaller than the mean shear stress (Duan and Barkdoll, 2006). This study adopted the assumption that bed shear stress satisfies a standard normal distribution. The porosity in Eq.14 could satisfy either the uniform distribution or the normal distribution. With those distributions of individual variables, the study assumed the probability density function of the coefficient of bank erosion satisfies either the normal distribution or the uniform distribution. The coefficient of bank erosion was first determined by calibrating the model using the observed data. The instantaneous coefficient of bank erosion at each bank was obtained from a random distribution function, which is based on the intrinsic function that produces random numbers between zero and one assuming a uniform or normal distribution. The Box and Muller (1958) transformation was used to convert the distribution from uniform to normal. This study simulated one thousand iterations for each distribution so as to

determine the statistical properties of the results including the 95 percent confidence interval and the average position of the stream centerline.

3. Results

3.1 Laboratory Experiment (Freidkin 1945)

A comprehensive laboratory study of river meandering was conducted at the Waterway Experiment Station, Army Corps of Engineers by J.F. Friedkin (1945). Among dozens of experimental runs, one began with a sine-generated initial channel of trapezoidal cross-sections, and uniform bed and banks, was run over several hours with a constant flow condition (see Plate 23 therein in Friedkin 1945). The constant discharge is 2.8 l/s, and the channel width is 0.40m with a side slope of 2:1. The total channel length is 12m. The experimental data, including flow velocity, channel slope, friction factor, Froude number, are summarized in Table 2. These experimental data are a unique opportunity to measure errors in the model with respect to the axial symmetry of the initial streamline. Plate 23 (Friedkin, 1945) was scanned and digitized with spatial reference given by the experimental figure in a geospatial database software (see Figure 3).

3.2 Simulated Results from Deterministic Model

The solutions of velocity excess from both models (Ikeda et al. 1981 and Johannesson and Parker, 1989b) in conjunction with Eq.1 were used to simulate the 32-hour experimental run. The simulated results were compared with the experimental measurements as shown in Figure 1 In the deterministic solution, with a constant value for $E = 2.2 \times 10^{-4}$, change in the channel centerline is driven by the excess velocity.

Figure 4 shows the results of excess velocity from both models, relative to the channel centerline. Line ‘a’ indicates the location of the minimum velocity excess which is slightly upstream of the inflection point of the streamline. Line ‘b’ in Figure 4 indicates the location of the maximum excess velocity which corresponds to the location along the outer bank across the point bar from the entrance to the bend. The maximum excess velocity occurs at the outer bank downstream of the apex. The maximum bank erosion occurs where the excess velocity is maximum.

Figure 5 graphs the difference between the experimental and modeled results of the maximum y-value or extent of lateral expansion of each bend, when beginning with a sine-generated curve and allowing the planform to evolve over 32 hours. The errors between the simulated and measured maximum distance from the x-axis are the y-values of nodes on the stream centerline were determined and shown in Figure 5. The Ikeda et. al. (1981) model has consistently smaller errors with the exception at the sixth bend. Over the first two bends, the Ikeda et. al. (1981) and Johannesson and Parker’s (1989b) models are consistent in their y-maximum value. Through the third and fourth bend, the models diverge, with Ikeda et. al.’s (1981) model over-predicting the lateral expansion at the third bend and under-predicting at the fourth bend, whereas the Johannesson and Parker (1989b) in the converse. Both models over-predict the maximum y-value at the sixth bend. Although no clear trend emerges, averaged values over all bends (see Table 4) shows that the Johannesson and Parker (1989b) model has significantly less average error.

Figure 6 illustrates the error in the model for the standard deviation of each bend comparing to the 32-hour streamline of the Friedkin (1945) experiment. Both models yielded the similar standard deviations from the mean y-value, and, therefore, the errors are of the same magnitude over the first and the second bend. The Johannesson and Parker (1989b) model consistently was a better predictor of the average y value and the standard deviation. Averaged values show slightly less error in the Johannesson and Parker (1989b) model.

Figure 7 shows the errors of skewness at each bend between the simulated results and the measurements. Both models yielded nearly identical results of the skewness, and were also of a similar magnitude. A great deal of variation exists in the observed data; however, both models yielded skewness values of the same sign and magnitude as the observed data. This phenomenon indicated the randomness of bank erosion and consequently, the meandering planform migration.

3.3 Simulated Results from Monte Carlo Simulation

If treating the coefficient of bank erosion as a random variable, a stochastic simulation is needed to accurately predict the evolution of meandering channels. Results illustrated from the deterministic models showed the MSE from the Ikeda et. al. (1981) model is less than that of the Johannesson and Parker (1989b) model. Other bend characteristics, however, indicated the Johannesson and Parker (1989b) model yielded better predictions of bend amplitude and skewness. This attribute supports the uncertainty in the coefficient of bank erosion used in the deterministic model. The Monte Carlo simulation using a stochastic coefficient of bank erosion is necessary. This study

represents the coefficient of bank erosion as a random variable and assumes its probabilistic density function satisfies either uniform or normal distribution. The linear bank coefficient used in the models is a proxy for the uncertainty associated with bank shear stress, soil composition, role of vegetation, and turbulence associated with bend flows. Figure 8 shows the results of the one thousand iterations given a 10% variation from the mean calibrated value used in the deterministic model.

By including all the y-values at each point along the stream line, the average y-value of the 1000 iterations and the 95% confidence interval can be determined. The results of both statistics are shown in Fig.9 for the Ikeda et. al. (1981) model, and in Fig.10 for the Johannesson and Parker (1989b). The errors of the maximum and standard deviation of y-values and skewness for each bend of the simulated stochastic mean channel were compared with the deterministic solutions in Figures 11, 12, and 13. With few exceptions, the average center streamline from the Monte Carlo simulation has less error than the deterministic solution. The one major exception is the prediction of the maximum y-value of the first and second bends (see Figure 11). Table 6 also shows that with the exception of the maximum y-value statistic the average values computed from the Monte Carlo simulation result in less error than the deterministic model solution.

Assuming normal and uniform distributions of the coefficient of bank erosion using Ikeda et. al.'s (1981) flow model, the results are shown in Fig. 14. Both distributions yielded nearly the same mean channel and slightly different 95% C.I. bounds. The measured channel centerline was within the 95% C.I. for both distributions.

This perhaps indicates that the distribution function of the coefficient of bank erosion has minor impacts on the mean simulated results.

4. Discussions

The computational expense associated with the additional complexity of the Johannesson and Parker (1989b) model do not significantly improve the overall model performance. This study showed that the simpler Ikeda et. al. (1981) model performed better using the cited performance metrics. Whereas other authors have reported modifying or merging the two models in unique ways (Wallick, 2006; Constantine, 2009, Camporeale et. al., 2007), and often reduced the complexity, this simulation used the full analytical solution found by Johannesson and Parker (1989b). A thorough review of the linear models presented herein, along with the non-linear counterparts is given by Camporeale et. al. (2007) and they found that the degree of complexity or simplifications should be commensurate with the peculiar characteristics of the problem under investigation. Figure 1 clearly indicates that the models do not produce a symmetric planform, despite a constant value of E. Authors have reported the need for significantly smoothing the stream centerlines, mainly by employing sequential cubic splines, and complex curvature calculations; neither of those were employed in this study which may have led to errors in velocity excess and, therefore, the estimation of planform evolution.

Modeling errors in simulating the evolution of river meandering is not trivial. Whereas the meandering planform is best described in the curvilinear coordinate, constraints such as the node placement and distances between nodes, and continuous phenomenon estimated in discrete spatial and temporal data sets, make direct comparison

difficult. Nevertheless, a variety of bend characteristics are of interest to describe the geometry of an evolving meandering river planform. The characteristics qualifying bend geometry include the lateral rate of expansion, the magnitude of rotation towards upstream or downstream, and the speed of bend upstream/downstream translation. The maximum y-value is clearly of interest because it measures the maximum lateral extension of the bend; however, this value in relation to the midpoint of the bend could be more interest to the modeler, which is an indicator of symmetrical geometry. The standard deviation of the y-values at each bend provides insight into how sharp or round the bend is. Therefore, the standard deviation is an excellent metric with which to compare the shape of bends. Bend skewness is a metric which provides meaningful measure of simulation error and aid in predicting planform evolution. Up- and down-stream rotation is captured through the skewness measure. Despite the fact flow field was solved in the curvilinear coordinate, the mean squared error of the simulated planform with respect to the observed data in the Cartesian coordinate is believed to be a good estimate of overall error in the model. In the case of a natural river where the x axis is not aligned with the downstream direction, the channel center axes orientation needs to be defined based on the alignment of each bend.

The Monte Carlo simulation of the evolution of the meander planform, using the linear equation for bank erosion is a practical and realistic tool. Because of the variety and profundity of uncertainties associated with the linear coefficient of bank erosion, E, representing those uncertainties within the modeling framework is critical. Regardless that the average y-values from the Monte Carlo simulation were better estimates of

observed data, the strength in this methodology lies in the ability to define confidence intervals within which the meandering planform evolves. Although the entire observed planform is not within those confidence intervals, the vast majority (over 90%) of that planform is found within the 95% confidence interval. Those areas not within the confidence intervals are almost exclusively in the upper portion of the laboratory stream. These first few bends are somewhat anomalous, as the upper stream was significantly influenced by the entrance boundary condition.

Figure 3 shows the evolution of the laboratory stream produced by Friedkin (1945). The relative equilibrium of that planform takes after just 32 hours. The subsequent planforms do not differ significantly in amplitude, skew, or translation, suggesting the stream has reached regime conditions and is in a state of dynamic equilibrium. Therefore, when calibrating to the 32-hour planform, those parameter values could not be used to predict future planforms, calling in to question the calibration using historical records often used with the linear model of bank erosion. These results suggest that a combination of those empirical models based on the overall meander river characteristics, flow, and sediment parameters, along with the linear bank erosion model using the Monte Carlo simulation is most appropriate to predict meandering channel evolution.

5. Conclusions

This paper reported one dimensional numerical simulation of meandering evolution using deterministic and stochastic models. The 1^{st} order solutions of Navier Stokes equation in the curvilinear coordinate by Ikeda et al. (1981) and Johannesson and Parker (1989b)

were used for determining the excess velocity. The rate of bank erosion is assumed linearly proportional to near bank excess velocity. The deterministic model adopted a constant coefficient of bank erosion for the entire simulation reach, whereas the stochastic model treated the coefficient of bank erosion as a random variable satisfying either uniform or normal distribution. For the deterministic model, Johannesson and Parker (1989b)'s model predicted better bend characteristics than the results of Ikeda et al. (1981)'s model although errors from both models exceeds 50%. This strongly suggested the limitation and incapability of deterministic models. On the other hand, the stochastic model yielded a 95% confidence interval bound that nearly bounds 90% of the observed channel centerline. The mean centerline from the stochastic model is within 30% errors when comparing to observed data. These results indicated that implementation of the Monte Carlo approach when using the suite of linear models is a more accurate representation of the evolution of the river planform and captures the variability associated with planform evolution and model error.

Acknowledgements

We thank Dr. Vince Tidwell of Sandia National Labs for ideas, assistance, and patience. We would also like to thank Dr. Hoshin Gupta for his help with the stochastic simulation and discussions of model structure. NSF Award EAR-0846523 is also appreciated for their support of Dr. Jennifer Duan. Support for this research was provided by Sandia National Labs through a partnership with the Department of Hydrology and Water Resources at the University of Arizona, Tucson, Arizona and the Sustainability of Semi-Arid Hydrology and Riparian Areas Research Center.

References

Box, G.E.P. and Mervin E. Muller, 1958. A Note on the Generation of Random Normal Deviates, The Annals of Mathematical Statistics, 29(2) pp. 610–611

Camporeale, C., Perona, P., Porporato, A., and Ridolfi, L., 2005. On the long term behavior of meandering rivers, Water Resour. Res., 41, W12403, doi:10.1029/2005WR004109.

Camporeale, C., Perona, P., Porporato, A., and Ridolfi, L., 2007. Hierarchy of models for meandering rivers and related morphodynamic processes. Rev. Geophys., 45, RG1001, doi:10.1029/2005RG000185.

Cheng N. and Law, A. W., 2003. Fluctuations of turbulent bed shear stress. J. Hydraul. Eng., 129(1), 126-130.

Constantine, C.R., Dunne, T., and Hanson, G.J., 2009. Examining the physical meaning of the bank erosion coefficient used in meander migration modeling. Geomorphology 106, 242- 252.

Crosato, A., 1990. Simulation of meandering river processes, communications on hydraulic and geotechnical engineering, Technical report, Civil Engineering Department, Delft University of Technology.

Darby, S.E., Thorne, C.R., 1994. Prediction of tension crack location and riverbank erosion hazards along destabilized channels. Earth Surf. Process. Land., 19, 233-245

Darby, S. E. and Thorne, C. R., 1996. Development and testing of riverbank-stability analysis. J. Hydraul. Eng., 122(8), 443-454.

Darby, S. E., Alabyan, A. M., Van De Wiel, M J., 2002. Numerical simulation of bank erosion and channel migration in meandering rivers. Water Resour. Res., 38(9), 2-1~2-12.

Duan, G. H., 1998. Simulation of alluvial channel migration processes with a two-dimensional numerical model, Dissertation, the Center for Computational Hydroscience and Engineering, the University of Mississippi, University, Mississippi.

Duan, J. G., 2001. Discussion of "numerical analysis of river channel processes with bank erosion", J. Hydraul. Eng., 127(8), 702-703.

Duan, J.G., 2005. Analytical approach to calculate the rate of bank erosion, J. Hydraul. Eng., 131(11), 980-990.

Duan, J.G. and Julien, P., 2005. Numerical simulation of the inception of meandering channel, Earth Surf. Process. Landf., 30, 1093-1110.

Duan, J. and Barkdoll, B., 2008. Surface-based fractional transport predictor: deterministic or stochastic, J. Hydraul. Eng., 134(3), 350-353.

Engelund, F., 1964. Flow resistance and hydraulic radius. ACTA polytechnic Scandinavia, Civ. and Engrg. Series, Ci 24, Copenhagen, Denmark, 1-23.

Engelund, F., 1974. Flow and Bed Topography in Channel Bends. J. Hydraul. Div., 100(11), 1631-1648.

Frascati, A., and Lanzoni, S. 2009. Morphodynamic regime and long-term evolution of meandering rivers, J. Geophys. Res., 114, F02002, doi:10.1029/2008JF001101.

Friedkin, J.F., 1945. A Laboratory Study of the Meandering of Alluvial Rivers. U.S. Army Engineers Waterways Experiment Station, Vicksburg, MS.

Gottlieb, L., 1976. Three-dimensional flow pattern and bed topography in meandering channels. Series Paper 11, Institute of Hydrodynamics and Hydraulic Engineering, Technical University of Denmark, Copenhagen, Denmark.

Hasegawa, K. and Ito, H., 1978. Computer simulations on meander channel changes. Proc., Hokkaido Branch, Japan Society of Civil Engineering, 34.

Hasegawa, K.,1989. Universal bank erosion coefficient for meandering rivers. J. Hydraul. Eng. 115, 744–765.

Hickin, E. J. and Nanson, G. C. 1975. The character of channel migration on the beatton river, northeast British Columbia, Canada. Geol. Soc. Amer. Bull. 86, 487-494.

Hooke, J.M. and Rohrer, W., 1979. Geometry of alluvial fans: Effect of discharge and sediment size. Earth Surf. Process. Land., 4, 147-166.

Ikeda, S., 1975. On secondary flow and bed profiles in alluvial curved open channels. Proceedings of the XVIth JAHR Congress, Sao Paolo.

Ikeda, S., Parker, G. and Sawai, K., 1981. Bend theory of river meanders: Part I, Linear development. J. of Fluid Mech., 112, 363-377.

Ikeda, S., and Nishimura, T., 1986. Flow and bed profile in meandering sand-silt rivers. J. Hydraul. Eng., 112(7), 5 62-579.

Imram, J., Parker, J. G. and Pirmez, C., 1999. A nonlinear model of flow in meandering submarine and subearial channels. J. Fluid Mech., 400, 295-331.

Johannesson, H., 1985. Computer Simulation migration of meandering rivers. Thesis presented to the Univeristy of Minnesota, at Minneapolis, in partial fulfillment for the degree of Master of Science.

Johannesson, H., and Parker, G., 1989a. Secondary flow in mildly sinuous channel. J. Hydraul. Eng., 115(3), 289-308.

Johannesson, H., and Parker, G., 1989b. Velocity redistribution in meandering rivers. J. Hydraul. Eng., 115(8), 1019-1039.

Kikkawa, H., Ikeda, S., and Kitagawa, A., 1976. Flow and Bed Topography in Curved Open Channels. J. Hydraul. Div., 102(9), 1327-1342.

Langbien, W.B. and Leopold, L.B., 1966. River Meanders- Theory of Minimum Variance. Physiographic and Hydraulic Studies of Rivers, Geologic Survey Professional Paper 422-H. 1966

Larsen, E.W., Greco, S.E., 2002. Modeling channel management impacts on river migration: a case study ofWoodson Bridge State Recreation Area, Sacramento River, California, USA. Environ. Manage. 30, 209–224.

Lopez, F. and Garcia, M. H., 1999. "Wall similarity in turbulent open channel flow." J. Engrg. Mech., 127(7), 789-796.

Micheli, E.R., and J.W. Kirchner, 2002. Effects of wet meadow riparian vegetation on streambank erosion. 1. Remote sensing measurements of streambank migration and erodibility. Earth Surf. Process. Land. 27, 627-639.

Micheli, E.R., Kirchner, J.W., Larsen, E.W., 2004. Quantifying the effects of riparian forest versus agricultural vegetation on river meander migration rates, central Sacramento River, California, USA. River Res. Appl. 20, 537–548.

Osman, A. M. and Thorne, C. R., 1988. Riverbank stability analysis. 1: Theory. J. Hydraul. Eng., 114(2), 134-150.

Parker, G., Sawai, K., and Ikeda, S., 1982. Bend theory of river meanders: Part II, Nonlinear deformation of finite-amplitude bends. J. Fluid Mech., 115, 303-314.

Parker, G., 1982. Stability of the channel of the Minnesota River near State Bridge No. 93, Minnesota," Project Report No. 205, St. Anthony Falls Hydr. Lab Univ. of Minnesota, Minneapolis, Minn., 33 pp.

Perucca, E., Camporeale, C. and Ridolfi, L., 2007. Significance of the riparian vegetation dynamics on meandering river morphodynamics, Water Resour. Res., 43, W03430, doi:10.1029/2006WR005234.

Pizzuto, J.E., Meckelnburg, T.S.,1989. Evaluation of a linear bank erosion equation.Water Resour. Res. 25, 1005–1013.

Seim H.E., Blanton J.O., Elston S.A., 2009. The effect of secondary circulation on the salt distribution in a sinuous coastal plain estuary: Satilla River, GA, USA. Continental Shelf Research, 29(1), 15-28.

Suga, K., 1963. On local scour at river bends. Tech. Memo Public Works Res. Inst., Min. of Const. Japan, 5(4).

Sun, T., Meakin, P., JØssang, T., and Schwarz, K., 1996. A simulation model for meandering rivers. Water Resour. Res., 32, 2937-2954.

Wallick, J.R., Lancaster S.T., and Bolte, J.P., 2006. Determination of bank erodibility for natural and anthropogenic bank materials using a model of lateral migration and observed erosion along the Willamette River, Oregon, USA. River Res. Applic. 22, 631-649.

Whiting, P. and Deitrich, W., 1993. Experimental Studies of bed topography and and flow patterns in large amplitude meanders. Water Resour. Res., 29, 3605-3514.

Zimmerman, C. & Kennedy, J. F., 1978. Transverse bed slope in curved alluvial streams. J. Hydraul. Div. 104(1), 33-48.

Zolezzi, G. & Seminara, G., 2001. Downstream and upstream influence in river meandering. Part 1. General Theory and application to overdeepening. J. Fluid Mech. 438, 183-211.

Table 1.
Migration Rate and Erodibility Summary (Micheli and Kirchner, 2006) with percent error.

Migration Rate(m a^{-1})	**Standard Error**	**Percent Error**
1.3	0.4	30.77%
1.5	0.1	6.67%
0.23	0.02	8.70%
0.25	0.01	4.00%
Erodibility $^{x}10^{-7}$		
0.58	0.02	3.45%
0.64	0.03	4.69%
3.7	0.5	13.51%
8.4	0.7	8.33%
	Average Percent Error	10.01%

Table 2. Friedkin Initial Conditions for Simulation

Parameter	**Value**
Initial Angle (degrees)	30.0
Wavelength (m)	6.4008
Bottom width (m)	0.3048
Side Slope (H:V)	1.0
Number of Wavelengths	5.0
Stream Flow (m^3/s)	2.83 X 10^{-3}
Stream Height (m)	0.027
Scour Factor (A)	2.89
Simulation Duration (hrs)	32
Erodibility Coefficient, E	2.2 X 10^{-4} (calibrated value)
Average Velocity (m/s)	0.339
Froude Number	0.65
Friction Factor	1.799 X 10^{-2}
Bed Slope	7.5 X 10^{-3}

Table 3
Model Error Statistics

	Statistic	**Interpretation**
Bend Characteristics	Maximum y-value	Maximum lateral extension
	Standard Deviation	Peakiness or flatness
	Skewness	Up- or downstream rotation

Total Streamline	Mean Squared Error	Y-value total error

Table 4
Average statistic error values of all planform bends for Ikeda (1981) and Johannesson and Parker (1989b) models.

Model	**Bend Average Error**		
	Ymax	Standard Deviation	Skewness
Ikeda (1981)	0.30297	0.265407	0.272529
Johannesson and Parker (1989b)	-0.0598	0.164785	0.211607

Table 5
Mean squared error values for Ikeda (1981) and Johannesson and Parker (1989b) models.

Model	**MSE**
Ikeda (1981)	3245.40558
Johannesson and Parker (1989b)	3426.20621

Table 6
Average statistic error values of all planform bends for Ikeda (1981) deterministic and stochastic solutions.

Model	**Bend Average Error**		
	Ymax	Standard Deviation	Skewness
Ikeda Deterministic (1981)	0.30297	0.265407	0.272529
Ikeda Stochastic	-0.44453	-0.08422	0.196721

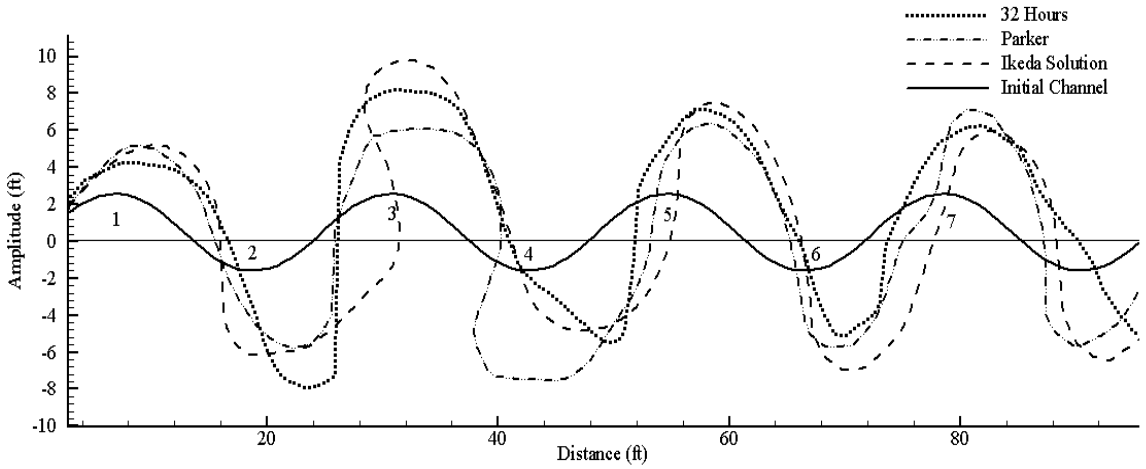

Fig. 1. Results of deterministic models Johannesson and Parker (1989b) and Ikeda (1981) for 32 hour simulation of J.R. Friedkin (1945) experimental results.

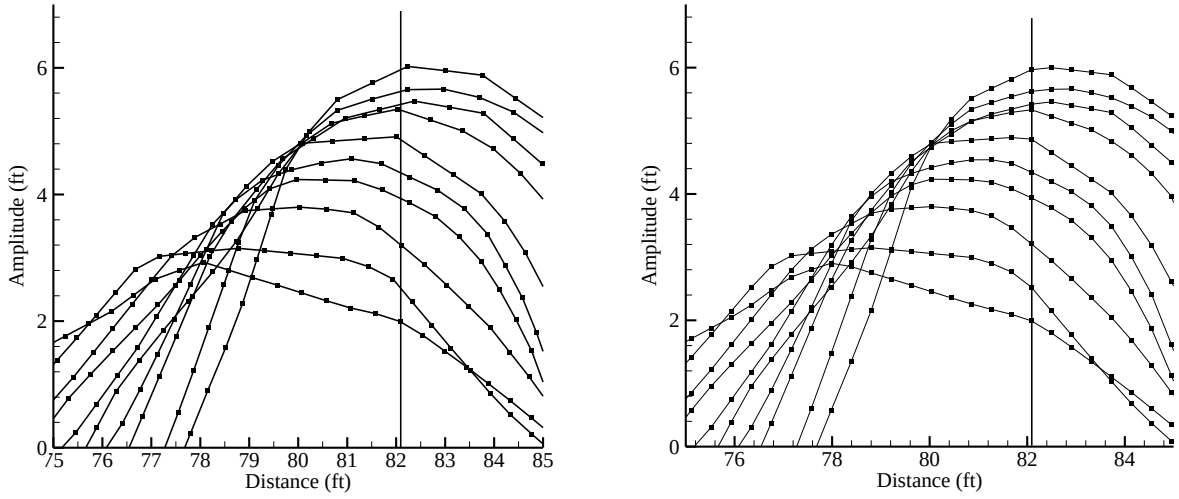

Fig. 2. Interpolation of computational nodes at discrete time intervals.

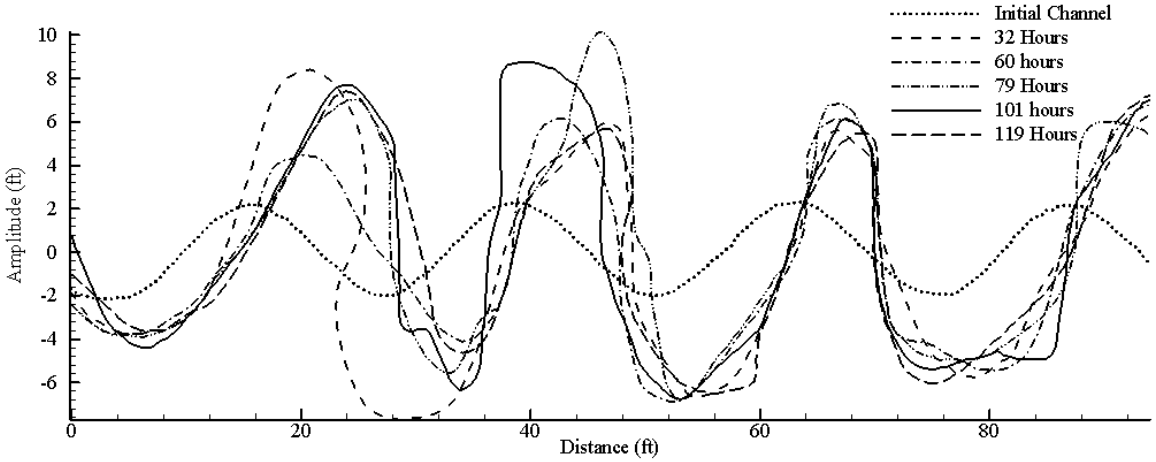

Fig. 3. Planform evolution of Friedkin (1945) experiments.

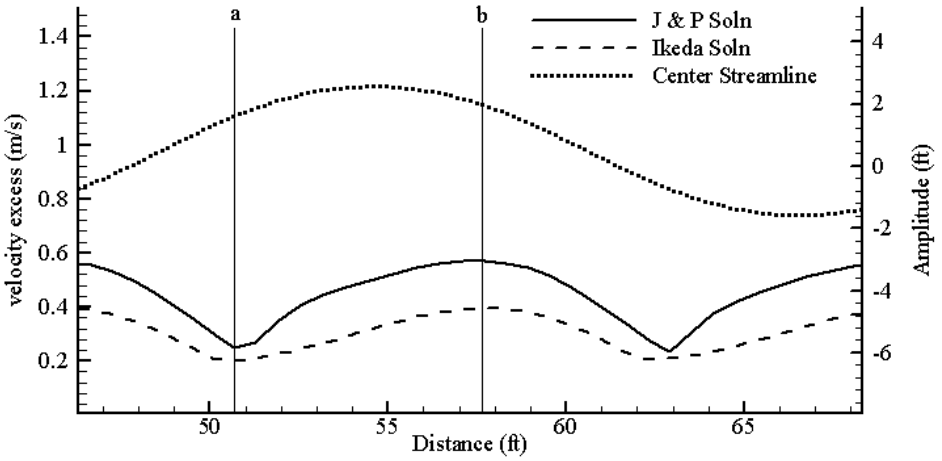

Fig. 4. Excess velocity results of flow field models Johannesson and Parker (1989b) and Ikeda (1981) for initial sine generated curve.

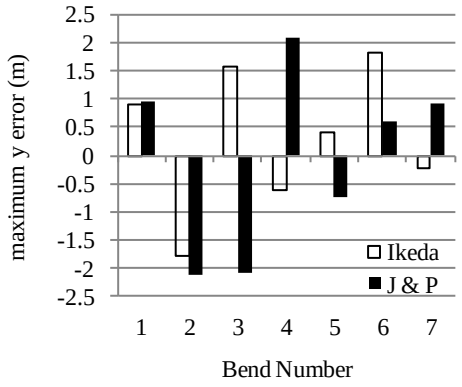

Fig. 5. Model error for distance from x-axis to maximum y-value for each bend simulated for 32 hour Friedkin (1945) simulation.

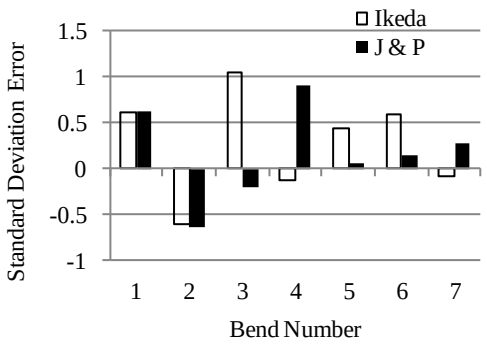

Fig. 6. Model error for deviation from the mean y-value for each bend simulated for 32 hour Friedkin (1945) simulation.

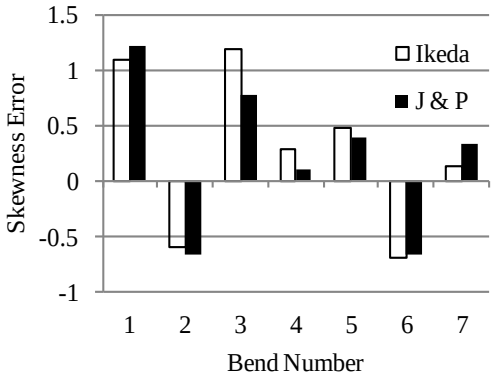

Fig. 7. Model error for skew of y-values for each bend simulated for 32 hour Friedkin (1945) simulation.

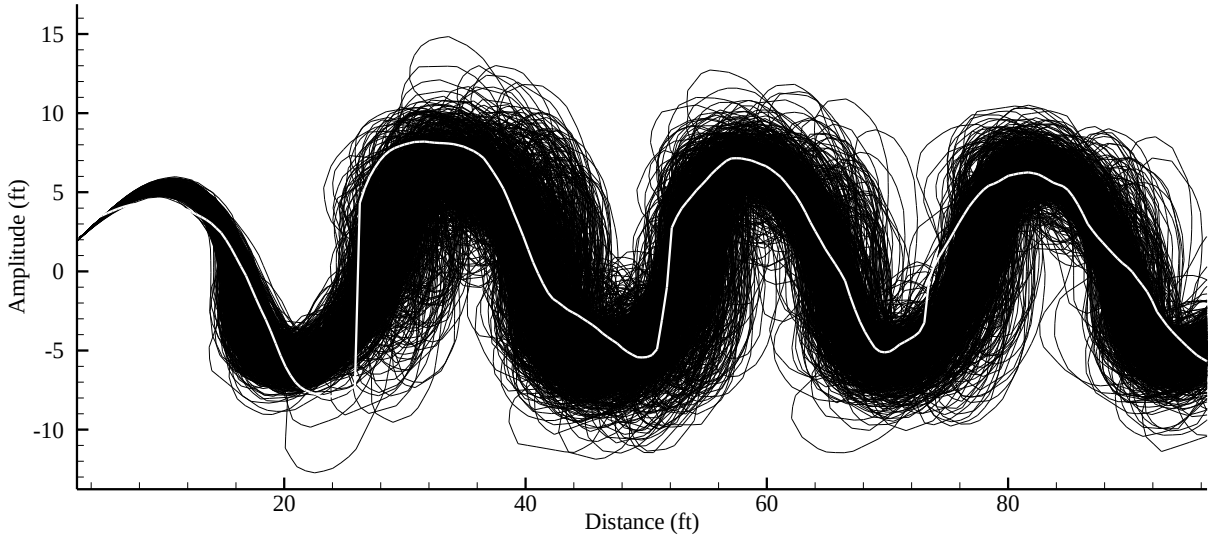

Fig. 8. 1000 iterations of Ikeda et. al. (1981) model with 10% variability from 32 hour calibrated value.

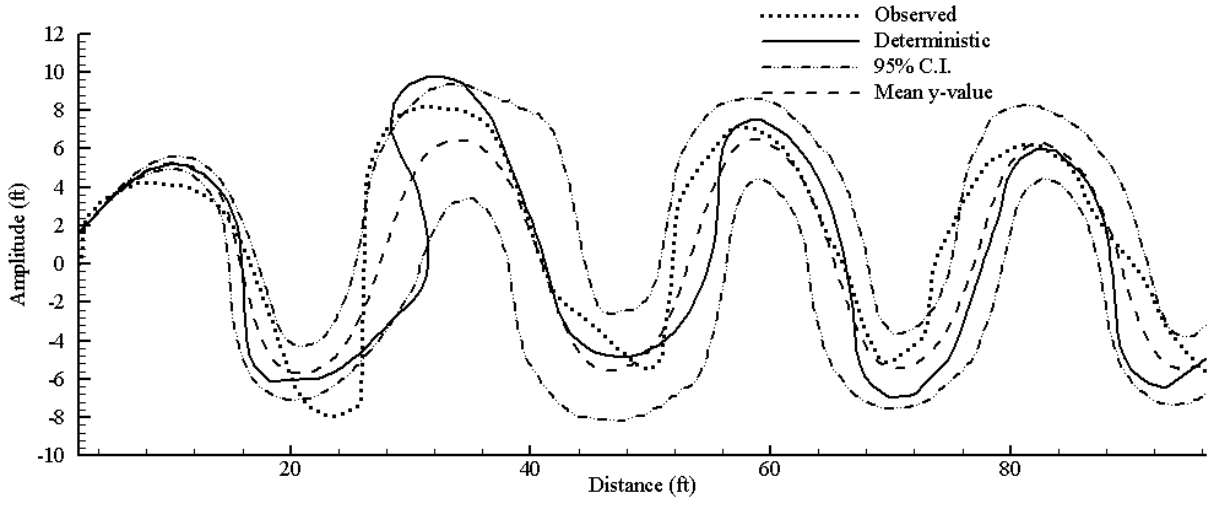

Fig. 9. Results of Monte Carlo analysis of 32 hour calibrated model with Ikeda (1981) solution.

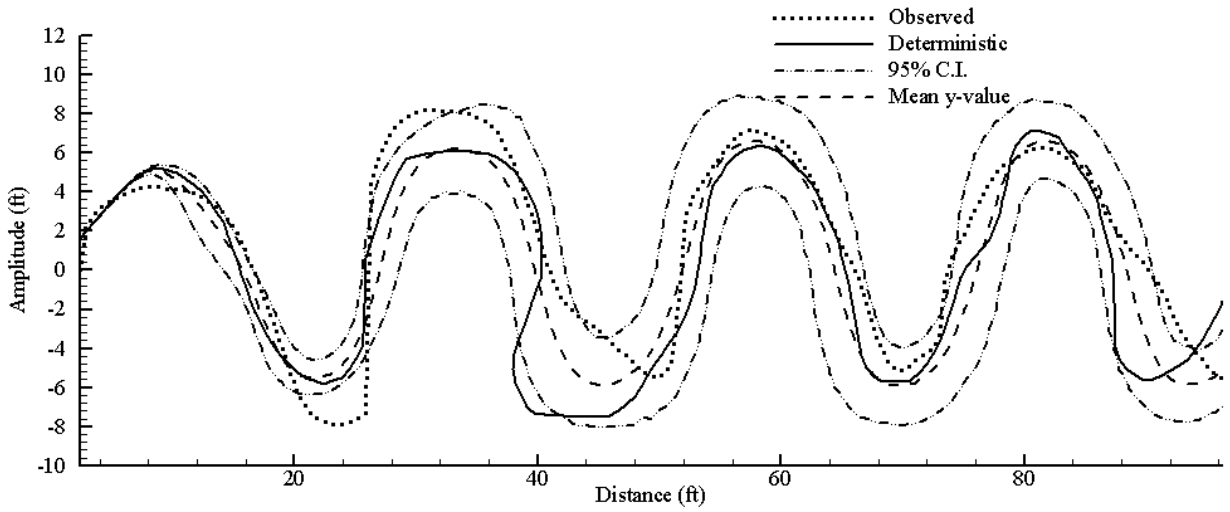

Fig. 10. Results of Monte Carlo analysis of 32 hour calibrated model with Johannesson and Parker (1989b) solution.

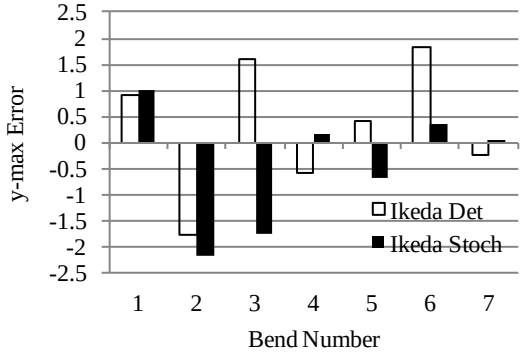

Fig. 11. Comparison of deterministic model and average y-max value from Monte Carlo simulation

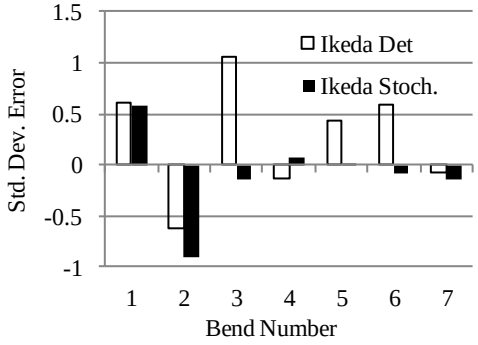

Fig. 12. Comparison of deterministic model and standard deviations of average y- value from Monte Carlo simulation

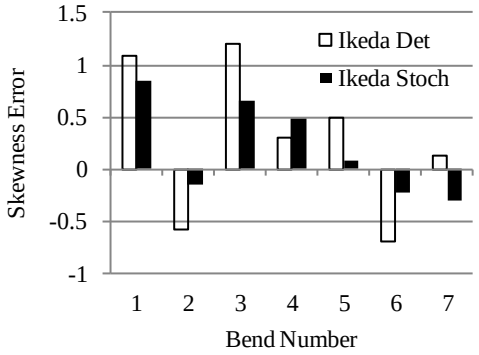

Fig. 13. Comparison of deterministic model and skewness of average y- value from Monte Carlo simulation.

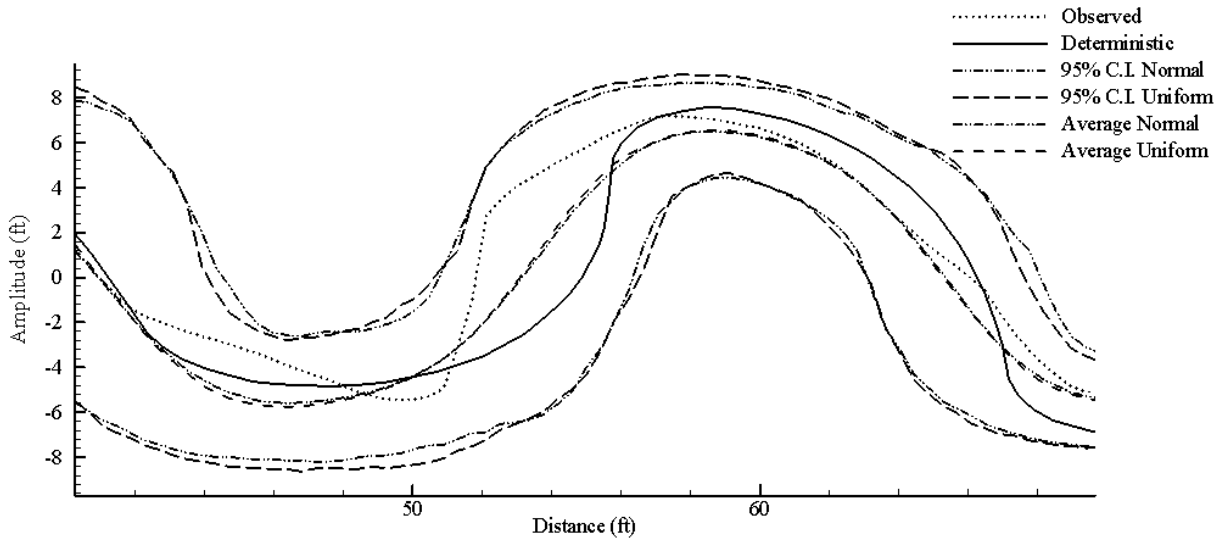

Fig. 14. Bends 4 and 5 of 32-hour simulation with results from both uniform and normal distributions.